standards are available commercially, the vendors do not guarantee long-term stability and accuracy.

Formaldehyde standards generally are prepared by one of several methods. The first method utilizes dilute commercial formalin (37% HCHO, w/w). Calibration is accomplished by the direct spiking into sampling impingers of the diluted mixture or by evaporation into known test volumes, followed by impinger collection. Formaldehyde also can be prepared by heating known amounts of paraformaldehyde, passing the effluent gases through a methanol-liquid nitrogen slush trap to remove impurities, and collecting the remaining HCHO. Paraformaldehyde permeation tubes also have been used (Tanner and Meng, 1984).

For the higher molecular weight carbonyl species, liquid solutions can be evaporated, or pure vapor can be generated in dynamic gas-flow systems (permeation tubes, diffusion tubes, syringe delivery systems, etc.). These test atmospheres are then passed through the appropriate collection system and analyzed. A comparison of these data, with the direct spiking of liquid carbonyl species into the particular collection system, provides a measure of the overall collection efficiency.

3.5.2.4 Polar Volatile Organic Compounds

The VOCs discussed earlier in this chapter (Section 3.5.2.2) have included aliphatic, aromatic, alkenic, and acetylenic hydrocarbons. These compounds are relatively nonpolar, nonreactive species, and measurement methods have been easily applied in determining ambient concentrations.

Recently, attention also has been directed toward the more reactive oxygen- and nitrogen-containing organic compounds, in part by the inclusion of many of these compounds on a list of 189 hazardous air pollutants specified in the 1990 CAAA (U.S. Congress, 1990). Many of these compounds are emitted directly from a variety of industrial processes, mobile sources, and consumer products, and some also are formed in the atmosphere by photochemical oxidation of hydrocarbons. However, as indicated earlier in this document, very few ambient data exist for these species. These compounds have been referred to collectively as PVOCs, although it is their reactivity and water solubility, more than simple polarity, that make their measurement difficult with existing methodology.

Two approaches have been utilized in developing analytical methods for PVOCs. One approach has incorporated the use of cryogenic trapping techniques similar to those discussed earlier for the nonpolar hydrocarbon species; the second approach has utilized adsorbent material for sample preconcentration. To be effective for sensitive parts-per-billion measurement of PVOCs, both approaches require some type of water management system to mitigate the adverse effects that water has on the chromatography and detector sensitivity and reliability. Several researchers have reported the use of cryogenic trapping with two-dimensional chromatography to selectively remove water vapor from the analytical process (Pierotti, 1990; Cardin and Lin, 1991). Although this column "heart cutting" technique has been successful for selected compounds, additional studies are needed to determine its potential use for the wide range of PVOCs. Ogle et al. (1992) developed a novel water management system based on the condensation of moisture from the saturated carrier gas stream during thermal desorption of a cryogenic trap. The moisture management system was found to be effective for reducing the amount of water delivered to the column during laboratory analyses of spiked mixtures. However, the system has not yet been extended to field monitoring. Gordon and Miller (1989) have used cryogenic trapping and

GC/MS spectrometry techniques to demonstrate the potential of chemical ionization (CI) within an ion trap to detect PVOCs. The water vapor present in the sample served as the CI reagent gas and appeared to be an effective reagent gas; however, deleterious chromatography results were also encountered. The authors concluded that further laboratory work is needed before this methodology can be applied to ambient air monitoring. Martin et al. (1991) also reported the use of cryogenic trapping with a GC-FID system to measure ambient levels of isoprene and two of its oxidation products, methacrolein and methylvinyl ketone (detection level of 0.5 ppb). The water vapor was selectively removed by using a potassium carbonate (K_2CO_3) trap ahead of the cryogenic trap. Frequent replacement of the K_2CO_3 trap was required.

The use of solid adsorbents for sample preconcentration of PVOCs has been reported by Kelly et al. (1993). The analytical method was used extensively at two field sites that formerly were used in EPA's Toxic Air Monitoring Study (TAMS). The analytical method consisted of GC separation of PVOCs with quantification by a ion-trap mass spectrometer. A two-stage adsorbent trap containing Carbopack B and Carbosieve S-III (Supelco catalog number 2-0321) was used to separate water vapor from the PVOCs. The optimum room temperature trapping and drying procedure consisted of a 320-cc sample (100 cc/min) followed by a dry nitrogen purge of 1,300 cc (100 cc/min). The trap was then backflushed and thermally desorbed with helium at 220 °C. A 5-min, 260 °C trap bakeout followed each collection-analysis cycle. The target list contained 14 PVOCs, including alcohols, ethers, esters, and nitrile species. Individual detection limits ranged from 0.2 to 1 ppb.

3.5.3 Sampling and Analysis of Nitrogen Oxides
3.5.3.1 Introduction
The measurement of NO_x in ambient air is of interest because of the role that certain of those compounds play as precursors to O_3 and because NO_2 has been shown to impact health effects. Most of the NO_x emitted from combustion sources are NO and NO_2. Collectively these two compounds are called NO_x. They contribute to O_3 formation by means of reactions discussed in Section 3.2. As a result, measurement of NO_x is important in efforts to understand and control O_3 and NO_2 in ambient air.

The atmospheric photochemistry that produces O_3 also results in conversion of NO and NO_2 to products such as HNO_3, nitrous acid (HNO_2), organic nitrates such as PAN ($CH_3C(O)O_2NO_2$), and other species. The total of all of these labile nitrogen species in air, NO_x included, is termed NO_y. Such compounds may be labile via photolysis (e.g., HNO_2) or thermal decomposition (e.g., PAN), and may be toxic, irritating, or acidic. The organic nitrates can occur in the atmosphere as reservoirs for NO_2. However, in general, they do not play the same critical role that NO_2 and NO play as O_3 precursors. For that reason, this section focuses on measurement methods for NO and NO_2, as the primary O_3 precursors of NO_x. Nitrogen oxides other than NO_x may be important, however, as interferents in efforts to measure NO and NO_2. These non-NO_x species are considered in this section in that regard.

Measurements of NO_x may involve measurements of NO, of NO_2, or of the sum of NO_x. Nitrogen dioxide, but not NO, is a criteria air pollutant, and, thus, reference and equivalent methods are specified for NO_2 measurements. In this section, the current state of measurement methods for NO and NO_2 will be summarized separately. Such methods in some cases rely on measurements of total NO_x, or at least an approximation of NO_x. This

discussion focuses on current methods and on promising new technologies, but no attempt is made here to cover the extensive history of the development of these methods. More detailed discussions of such methods may be found elsewhere (U.S. Environmental Protection Agency, 1993c; National Aeronautics and Space Administration, 1983). Wet chemical methods are no longer commonly used and are not discussed here; a review of such methods is given by Purdue and Hauser (1980).

3.5.3.2 Measurement of Nitric Oxide
Gas-Phase Chemiluminescence Methods

By far the most common method of NO measurement is gas-phase CL with O_3. In this method, excess O_3 is added to air containing NO in a darkened, internally reflective chamber monitored by a photomultiplier tube. A small portion of the NO reactions with O_3 produce electronically excited NO_2 molecules that decay by emission of light of wavelengths longer than 600 nm. The emitted light is detected by a red-sensitive photomultiplier tube, through an optical filter that prevents passage of wavelengths shorter than 600 nm. This optical filtering minimizes interference from CL produced by O_3 reactions with other species (e.g., hydrocarbons). The excited NO_2 is readily quenched in air, so that, in typical instruments, air and O_3 are mixed at reduced pressure (i.e., at least 20 in. of Hg vacuum). The intensity of the emitted light is linearly proportional to the NO content of the sample air over several orders of magnitude in concentration.

Commercial CL instruments for continuous measurement of NO are available from several manufacturers. The chemiluminescence approach is also an EPA-designated measurement principle for measuring ambient NO_2; it requires a means of converting NO_2 to NO for detection. The complexities of this conversion are discussed in Section 3.5.3.3, on NO_2 methods. The commercial NO monitors typically are claimed to have detection limits of a few parts per billion by volume in air, with response time of a few minutes. Field evaluations of several commercial instruments have indicated that minimum levels of detection for NO_2 are 5 to 13 ppbv (Michie et al., 1983; Holland and McElroy, 1986). However, more recent evaluations have indicated better performance. Rickman et al. (1989) reported detection limits of 0.5 to 1 ppbv, and precision of ±0.3 ppbv, from laboratory and field evaluations of two commercial instruments operated on their 50 ppbv full-scale ranges. Commercial NO analyzers are portable and quite reliable and now are commonly used in ambient air monitoring networks.

Commercial NO analyzers may not have sensitivity sufficient for surface measurements in urban, rural, or remote areas, or for airborne measurements. As a result, several investigators have devised modifications to commercial instruments to improve their sensitivity and response time (Delany et al., 1982; Tanner et al., 1983; Dickerson et al., 1984; Kelly et al., 1986). Those modifications include operating at low pressure and high sample flow rate; using a larger, more reflective reaction chamber that promotes mixing of the reactants close to the photomultiplier tube; increasing the O_3 supply; for example, by use of oxygen in the O_3 source; cooling of the photomultiplier to reduce noise; adopting photon-counting techniques for light detection; and adding a prereactor to obtain a more stable and appropriate background signal. Commercial instruments modified in these ways are generally reported to have detection limits of 0.1 ppbv or less, with response times of 30 s or less.

Research-grade NO instruments specially designed for ultra-high sensitivity also have been built for use in remote ground-level or airborne applications (e.g., Ridley and

Howlett, 1974; Kley and McFarland, 1980; Kelly et al., 1980; Helas et al., 1981; Drummond et al., 1985; Torres, 1985; Kondo et al., 1987; Parrish et al., 1990). These instruments typically have detection limits of 10 ppt (i.e., 0.01 ppbv) or less, with response times from a few seconds to 1 min.

A number of studies indicate that the CL method is essentially specific for NO. Operation at reduced pressure prevents interference resulting from quenching by water vapor (Michie et al., 1983; Drummond et al., 1985). In air sampling, no significant interferences have been found in NO detection from sulfur-, chlorine-, and nitrogen-containing species (Joshi and Bufalini, 1978; Sickles and Wright, 1979; Grosjean and Harrison, 1985b; Fahey et al., 1985). However, H_2S and possibly other sulfur-containing compounds from seawater have been reported to give false NO signals (Zafiriou and True, 1986). This effect should not be important for ambient air measurements. Fahey et al. (1985) and Drummond et al. (1985) also reported no significant NO interference from a variety of other nitrogen-containing species, including NO_2, HNO_3, PAN, N_2O_5, NH_3, HCN, N_2O, and HO_2NO_2; as well as no interference from CH_4, propylene, and H_2O_2.

Several ambient air intercomparisons have been done of CL NO instruments (Walega et al., 1984; Hoell et al., 1987; Fehsenfeld et al., 1987; Gregory et al., 1990a). These studies have focused on high-sensitivity research instruments, rather than the commercial instruments used for widespread ambient air measurements. These studies have shown excellent agreement among the CL NO instruments, even at NO levels in the low ppt range (Hoell et al., 1987; Gregory et al., 1990a). These results support the validity of the CL approach for NO. Good agreement also has been found between CL measurements and spectroscopic NO measurements in these studies (see Section 3.5.3.2).

Spectroscopic Methods for Nitric Oxide

Direct spectroscopic methods for NO include two-photon laser-induced fluorescence (TPLIF), TDLAS, and two-tone frequency-modulated spectroscopy (TTFMS). The primary characteristics of these methods are their very high sensitivity and selectivity for NO. For example, a detection limit of 10 ppt has been quoted for TPLIF with a 30-s integration time, with no significant interferences from atmospheric species (Davis et al., 1987). An accuracy of ±16% as a 90% confidence limit has been calculated for NO measurement by TPLIF from an aircraft (Davis et al., 1987). The TDLAS method is similarly highly selective for NO and achieves a detection limit of 0.5 ppbv (Schiff et al., 1983). The response time of the TDLAS instrument is about 1 min for NO, and is limited by stabilization of concentrations with the large surface area of the multi-pass White cell. The newest method is TTFMS, which appears in laboratory studies to be very sensitive, fast, and selective. With a 100-m path length in a 20-torr multiple-pass cell, and a 1-min averaging time, the detection limit of NO is estimated to be 4 ppt (Hansen, 1989).

Spectroscopic methods have compared well with the CL method for NO in ambient measurements. Walega et al. (1984) reported good agreement between CL and TDLAS results for NO in laboratory air, in ambient air, and in downtown Los Angeles air. Gregory et al. (1990a) reported comparisons of TPLIF and CL NO methods in airborne measurements. Agreement at levels below 20 ppt was within the expected accuracy and precision of the instruments (i.e., within 15 to 20 ppt).

The major drawbacks of these spectroscopic methods are their complexity, size, and cost. Although possessing remarkable characteristics, these methods are restricted to

research applications. The TTFMS approach, in fact, is still in the laboratory development stage.

Passive Samplers

At present, no passive sampler exists that directly measures NO. Instead, passive samplers developed for NO_2 have been adapted for NO measurement, using an oxidizing material that converts NO to NO_2. Palmes tubes (Palmes and Tomczyk, 1979) have been adapted for NO measurement by using two tubes in parallel. One tube collects NO_2 on a triethanolamine (TEA)-coated grid, whereas the other collects NO_2 on a TEA grid, plus NO oxidized by a chromic acid-coated surface. The grids are then extracted and analyzed for NO_2^- ion. Nitric oxide is determined by difference between the two results, after accounting for the different diffusivities of NO and NO_2. The sampling rates depend on temperature and air velocity. The tubes cannot be used for periods longer than 24 h and are intended for use at ppm NO levels important in the workplace (e.g., 2 to 200 ppm $\cdot$ h). Applicability to ambient NO levels has not been demonstrated.

A more sensitive passive sampler for NO has been reported (Yanagisawa and Nishimura, 1982) that uses the same TEA chemistry, with CrO_3 as the NO oxidizer. A detection limit of 70 ppbv-h has been reported. As with any currently available passive sampler, the disadvantages of the method are the potential for interferences, relatively poor precision, and low sensitivity for ambient air measurements.

3.5.3.3 Measurements for Nitrogen Dioxide
Gas-Phase Chemiluminescence Methods

In 1976, the gas-phase CL approach described above for NO detection was designated as the measurement principle on which EPA reference methods for ambient NO_2 must be based. The CL method thus filled the vacancy left by withdrawal of the Jacobs-Hochheiser method, because of technical problems, in 1973. To be designated as a reference method, an NO_2 detection method must use the CL approach and be calibrated by the specified methods (gas-phase titration of NO with O_3, or use of an NO_2 permeation device). In addition the instrument must meet the performance specifications shown in Table 3-18. An equivalent method, either manual or automated, must meet certain requirements for comparability with a reference method when measuring simultaneously in a real atmosphere. Those comparability requirements are shown in Table 3-19. An automated equivalent method must also meet the performance requirements shown in Table 3-18.

The selection of the O_3-CL method as the reference measurement principle for ambient NO_2 was the result of comparison tests of CL and wet chemical methods. Chemiluminescence analyzers were found superior to the wet chemical methods in response time, zero and span drift, and overall operation, although agreement among all the methods tested was good, at the NO_2 spike levels provided (Purdue and Hauser, 1980). Table 3-20 lists the methods currently designated (as of August 1, 1994) by EPA as reference and equivalent methods for ambient NO_2. Three wet chemical methods are shown as equivalent methods, but these rarely are used for ambient air measurements.

The O_3 CL method does not measure NO_2 directly, because the CL is produced by reaction of NO with O_3. As a result, NO_2 must first be reduced to NO for detection. In principle, such a reduction should readily result in measurement of NO + NO_2 (i.e.,

Table 3-18. Performance Specifications for Nitrogen Dioxide Automated Methods[a]

Performance Parameter	Units	NO_2
Range	ppm	0-0.5
Noise		
0% Upper range limit	ppm	0.005
80% Upper range limit	ppm	0.005
Lower detectable limit	ppm	0.01
Interference equivalent		
Each interferant (SO_2,NO,NH_3,H_2O)	ppm	±0.02
Total interferant	ppm	≤0.04
Zero drift, 12 and 24 hours	ppm	±0.02
Span drift, 24 hours		
20% Upper range limit	%	±20.0
80% Upper range limit	%	±5.0
Lag time	min	20
Rise time	min	15
Fall time	min	15
Precision		
20% Upper range limit	ppm	0.02
80% Upper range limit	ppm	0.03

[a]See Appendix A for abbreviations and acronyms.

Source: Code of Federal Regulations (1987), Ambient Air Monitoring Reference and Equivalent Methods, C.F.R. Title 40, Part 53.

Table 3-19. Comparability Test Specifications for Nitrogen Dioxide

Nitrogen Dioxide Concentration Range (ppm)		Maximum Discrepancy Specification (ppm)
Low	0.02 to 0.08	0.02
Medium	0.10 to 0.20	0.02
High	0.25 to 0.35	0.03

NO_x), and allow indirect measurement of NO_2 by difference between NO and NO_x responses, measured either sequentially, or simultaneously by separate detectors. In practice, however, selective measurement of NO_x by this approach has proven very difficult.

Several methods have been employed to convert NO_2 to NO, including catalytic reduction with heated molybdenum or stainless steel, reaction with CO over a gold catalyst surface, reaction with ferrous sulfate ($FeSO_4$) at room temperature, reaction with carbon at 200 °C, and photolysis of NO_2 at wavelengths of about 320 to 400 nm (Kelly et al., 1986). It has been found in many separate investigations that the heated converters reduce NO_2 to

Table 3-20. Reference and Equivalent Methods for Nitrogen Dioxide Designated by U.S. Environmental Protection Agency[a]

Method	Designation Number	Method Code
Reference Methods (Continuous CL Analyzers)		
Advanced Pollution Instrumentation 200	RFNA-0691-082	082
Beckman 952A	RFNA-0179-034	034
Bendix 8101-B	RFNA-0479-038	038
Bendix 8101-C	RFNA-0777-022	022
CSI 1600	RFNA-0977-025	025
Dasibi 2108	RFNA-1192-089	089
Lear Siegler ML9841	RFNA-1292-090	090
Meloy NA53OR	RFNA-1078-031	031
Monitor Labs 8440E	RFNA-0677-021	021
Monitor Labs 8840	RFNA-0280-042	042
Monitor Labs 8841	RFNA-0991-083	083
Philips PW9762/02	RFNA-0879-040	040
Thermo Electron 14B/E	RFNA-0179-035	035
Thermo Electron 14D/E	RFNA-0279-037	037
Thermo Environmental 42	RFNA-1289-074	074
Equivalent Methods (Wet Chemical)		
Sodium arsenite	EQN-1277-026	084
Sodium arsenite/Technicon II	EQN-1277-027	084
TGS-ANSA[b]	EQN-1277-028	098

[a]As of August 1, 1994.
[b]Triethanolamine-guaiacol-sulfite with 8-amino-1-naphthalene-sulfonic acid ammonium salt.

NO effectively, but also reduce other NO_y species as well (e.g., Winer et al., 1974; Cox, 1974; Joseph and Spicer, 1978; Grosjean and Harrison, 1985b; Fahey et al., 1985). Efficiencies of conversion near 100% are reported in these studies for NO_2 and for NO_y species such as HNO_3, HNO_2, PAN, and organic nitrates. This finding is particularly important for widespread monitoring networks that use commercial instruments, because such instruments without exception use heated catalytic converters (typically molybdenum). Thus, such instruments measure not NO and NO_x, but more nearly NO and total NO_y. Although NO_x is the predominant NO_y species during early morning hours, other NO_y species constitute a substantial percent of the NO_y later in the day, especially in rural areas. The NO_2 value inferred from such measurements may be significantly in error (see below), and may in turn affect the results of models of ambient O_3. The completeness of the measured NO_y value is also questionable because, for example, HNO_3 is readily lost to surfaces, and, in ambient sampling, may be removed within the sampling system before reaching the heated converter.

Other conversion methods for NO_2 have been tried in an effort to achieve higher selectivity. Ferrous sulfate has been used for ambient NO_2 measurements using high-sensitivity research grade CL instruments (e.g., Kelly et al., 1980; Helas et al., 1981; Dickerson et al., 1984). This material is an efficient reducer of NO_2, but also has been found to convert a portion of PAN, and possibly a portion of HNO_2 and organic nitrates (Fehsenfeld et al., 1987). Memory effects and reduction in efficiency can occur because of humidity effects (Fehsenfeld et al., 1987). As a result of these characteristics, use of $FeSO_4$ has given high readings in comparison with spectroscopic instruments and the photolytic NO_2 converter, and its use likely results in overestimating ambient NO_x by a significant amount (Fehsenfeld et al., 1987; Ridley et al., 1988a; Gregory et al., 1990b). Ferrous sulfate has never been used in commercial NO_x instruments and is no longer used in research measurements.

The most specific method for converting NO_2 to NO is photolysis (Kley and McFarland, 1980). In the most common approach, ambient NO_2 is photolyzed to NO by light of 350 to 410 nm from a xenon arc lamp. The method does not produce NO from the major potential interferents present in air (i.e., HNO_3, PAN, and organic nitrates), but less abundant NO_y species such as HNO_2 or HO_2NO_2 may interfere. A detailed description of steps to minimize such interferences is given by Ridley et al. (1988b). As currently used, the photolytic converter appears to be essentially specific for NO_2. However, it does not provide complete conversion of NO_2. Conversion efficiencies are 50 to 60% with a new lamp but may decline to 20% over the course of several weeks (Parrish et al., 1990). Thus, the conversion efficiency must be calibrated repeatedly. This approach has not been implemented with commercial NO detectors but has been implemented with research-grade CL NO instruments for studies of NO_x and NO_y chemistry at a variety of locations (e.g., Buhr et al., 1990; Parrish et al., 1990; Trainer et al., 1991; Parrish et al., 1992, 1993). The photolytic method compares well with other techniques, including spectroscopic methods, even at NO_2 levels as low as 0.05 ppbv (Gregory et al., 1990b). Further improvement of the photolytic converter approach is continuing. Bradshaw et al. (1994) reported on plans to minimize wall effects in the photolytic converter and to use a metal halogen lamp in place of the xenon arc lamp. The metal halogen lamp emits strongly in the proper wavelength region and is much less expensive than the xenon arc lamp, allowing more frequent replacement of the lamp and consequently higher long-term photolytic efficiency.

As noted above, the commercial CL analyzers used for most ambient air NO and NO_x measurements actually measure NO and NO_y. The magnitude of the resulting overestimation of NO_2, determined by difference, obviously depends on the portion of NO_y that is NO_x. The smaller the portion of NO_y that is NO_x, the greater will be the error in the NO_2 determined by difference. In rural/remote areas, where NO_x has undergone extensive conversion to other products during transport from a source region, NO_x may contribute a small fraction of NO_y. In urban areas, close to sources, NO_x may comprise nearly all of NO_y. For example, in measurements at Point Arena, Parrish et al. (1992) report NO_x/NO_y ratios averaging 0.3 in air of marine origin and 0.75 in air subject to continental influence. Buhr et al. (1990) and Parrish et al. (1993) reported measurements at rural sites in eastern North America that indicate NO_x/NO_y ratios ranging from about 0.25 to 0.75, varying with the time of day, with the lowest ratios occurring during daytime, photochemically active periods. Clearly, although the commercial CL instruments are designated as reference methods for NO_2, the great majority of existing ambient air data for NO_2 or NO_x are biased high, due to the inclusion of some portion of other NO_y species. The magnitude of this bias may not be large in urban areas, but, in any case, it is essentially unknown at this time.

Luminol Chemiluminescence Method

This approach is based on the CL reaction of gaseous NO_2 with the surface of an aqueous solution of luminol (5-amino-2,3-dihydro-1,4-phthalazinedione). Emission occurs primarily between 380 and 520 nm. In commercial instruments, luminol solution flows down a fabric wick that lies vertically on a clear window viewed by a photomultiplier tube. Nitrogen dioxide in sample air passing over the wick produces light, the intensity of which is proportional to the NO_2 concentration. Commercial instruments using this approach are compact, light, and relatively inexpensive and can provide detection limits as low as 0.01 ppbv, with response times below 30 s. The instrument has the advantage of detecting NO_2 directly. However, several difficulties have had to be dealt with in developing the method.

Original reports of the approach (Maeda et al., 1980) indicated positive interferences from O_3 and SO_2 and a negative one from CO_2. Reformulation of the luminol reagent solution has minimized, although not fully eliminated, those interferences (Wendel et al., 1983; Schiff et al., 1986). Reported effects include a slight negative response from NO, and sensitivity to PAN, HNO_2, and O_3 (Wendel et al., 1983; Schiff et al., 1986; Rickman et al., 1989; Kelly et al., 1990; Spicer et al., 1991). Response to NO_2 may be nonlinear at low concentrations (Kelly et al., 1990), although recent reformulation of the reagent apparently has reduced this behavior (Busness, 1992). Evaluation of the luminol NO_2 monitor indicates that great care must be taken in using and calibrating the instrument in order to achieve good precision and accuracy in ambient measurements (Kelly et al., 1990). The monitor has been used widely as a research tool, but has not been used widely in ambient air monitoring nor has it been designated an equivalent method for NO_2.

An O_3 scrubber is available to eliminate the O_3 interference noted above, but it also was found to remove a portion of the NO_2 (Kelly et al., 1990). The luminol approach also has been modified to measure NO, by using a CrO_3 converter that oxidizes NO to NO_2 for detection. Thus NO is detected by difference. This method has the potential for measurement of total NO_x; however, evaluations of the CrO_3 converter are still underway at several laboratories. Given the known interferences in the luminol approach, careful evaluation of this method must be completed before it gains acceptance as an NO measurement method.

An adaptation of the commercial luminol NO_2 detector has been reported to provide measurements of total NO_y, NO_2, and NO_x (Drummond et al., 1992). This adaptation, called the LNC-3M, uses a commercial luminol instrument for NO_2 detection, with a CrO_3 converter for NO_x detection. The NO_x measurement must be corrected for the few percent of the ambient NO_2 that is lost in the CrO_3 converter (Drummond et al., 1992). The NO_y measurement is achieved using a stainless steel converter maintained at 400 °C. Tests indicate that this converter provides a more complete conversion of alkyl nitrates, and consequently a more complete measurement of NO_y, than is provided by either the heated molybdenum converters used in commercial O_3 CL NO_x detectors or the gold converters with CO addition used in research instruments (Drummond et al., 1992). The LNC-3M adds a small amount of NO_2 to the sample to eliminate the nonlinearity at low concentrations, and uses a zeroing scrubber that greatly reduces the interference from PAN. However, this scrubber must be replaced weekly when it is in continuous use (Drummond et al., 1992).

Spectroscopic Methods

Several spectroscopic approaches to NO_2 detection have been developed; TDLAS, TTFMS, DOAS, and differential absorption lidar (DIAL) are absorption methods that have been used. The TDLAS method is probably the most commonly used spectroscopic NO_2 method. It can provide high selectivity for NO_2, with a detection limit of 0.1 ppbv, accuracy of ±15%, and a response time on the order of 1 min because of the White cell (Mackay and Schiff, 1987b). The DOAS method is an open-path, long-pathlength system. The detection limit for NO_2 with a 0.8-km pathlength and 12-min averaging time has been reported as 4 ppbv, with measurement accuracy reported as ±10% (Biermann et al., 1988). However, recent improvements have resulted in a commercial DOAS instrument capable of an NO_2 detection limit of 0.6 ppbv, based on a 557-m path and a 1-min averaging time (Stevens et al., 1993). The detection limit for NO_2 by the DIAL technique has been reported as 10 ppbv with a 6-km pathlength (Staehr et al., 1985). The novel TTFMS method noted above for NO is reported to have an NO_2 detection limit of 0.3 ppt, but is not fully proven for ambient measurements.

Fluorescence methods also have been used for NO_2, including photofragmentation TPLIF (PF/TPLIF) (Davis, 1988). This method uses two cells in which NO is measured by TPLIF. In one of the cells, an excimer laser emitting at 353 nm photolyzes NO_2 to NO for detection. Thus NO_2 is ultimately measured, by difference, as NO, but the NO is formed directly by photolysis of NO_2. With a 2-min integration time, an NO_2 detection limit of 12 ppt is reported. The method is highly selective for NO_2, because an interferant would have to photolyze to produce NO. Several potential atmospheric species have been ruled out in this regard (Davis, 1988).

The drawbacks of most of these methods are, as noted earlier, complexity, size, and cost. At present, these factors outweigh the obvious advantages of the sensitivity and selectivity of these spectroscopic methods and largely have restricted the use of these NO_2 methods to specific research applications or as reference methods in intercomparisons. In such intercomparisons, absorption measurements have been used most commonly. The TDLAS method has been used in ground-level comparisons with O_3 CL and luminol instruments to provide specific NO_2 measurements (Walega et al., 1984; Sickles et al., 1990; Fehsenfeld et al., 1990) and in an airborne comparison with PF/TPLIF and O_3 CL instruments (Gregory et al., 1990b). A finding of these studies was that the TDLAS consistently read higher than other established methods at very low NO_2 levels (i.e., <0.4 ppbv) (Fehsenfeld et al., 1990; Gregory et al., 1990b).

The spectroscopic NO_2 method most fully developed beyond the research stage is the DOAS technique. Stevens et al. (1993) report testing of a commercial DOAS instrument in North Carolina over 17 days in the fall of 1989. The DOAS measured NO_2 using wavelengths between 400 and 460 nm and achieved a detection limit of 0.6 ppbv, as noted above. Simultaneous measurements of O_2, SO_2, HCHO, and HNO_2 also were provided by the DOAS instrument. Comparison of the DOAS NO_2 results to those from a commercial CL detector showed (DOAS NO_2) = 1.14 × (CL NO_2) + 2.7 ppbv, with an r^2 of 0.93, at NO_2 levels up to 50 ppbv (Stevens et al., 1993). The sensitivity, stability, response time, and multicomponent capability are the primary advantages of the DOAS approach. Further intercomparisons and interference tests are recommended (Stevens et al., 1993).

Passive Samplers

Passive samplers are attractive, inexpensive, and simple means to obtain long-term or personal exposure data for NO_2 or NO_x. The simplest passive sampler for NO_2 is the nitration plate, which is essentially an open dish containing filter paper impregnated with TEA. Nitrogen dioxide diffuses to the paper and is extracted later as NO_2^- for analysis. No diffusion barrier exists in this approach or in a similar approach using a candle-shaped absorber (Kosmus, 1985). Consequently, results are very much subject to ambient conditions and give, at best, a qualitative indication of NO_2 or NO_x.

Addition of a diffusion barrier to the nitration plate concept has led to badge-type passive samplers for NO_2 (e.g., Mulik and Williams, 1986, 1987; Mulik et al., 1989, 1991). In general, such devices use perforated screens, plates, or filters as diffusion barriers on the chemically reactive material, which may be exposed on one or both sides, depending on the application. Extraction of the sorbent then allows measurement of the NO_2 collected, typically as NO_2^- ion. Such a device using TEA as the active material gave very good agreement relative to a CL analyzer in laboratory tests with NO_2 at 10 to 250 ppbv (Mulik and Williams, 1987). However, interferences from PAN and HNO_2 (the latter in both outdoor and indoor air) are expected (Sickles and Michie, 1987). Comparison of ambient NO_2 results in the 5 to 25 $\mu g/m^3$ range (i.e., about 2.5 to 12.5 ppbv) from the passive device to those from TDLAS showed good agreement on average values, but a correlation coefficient (r) of only 0.47 on daily values (Mulik et al., 1989).

Badge-type personal samplers for NO_2 also have been developed by Yanagisawa and Nishimura (1982) (YN) and by Cadoff and Hodgeson (1983) (CH). Triethanolamine is used as the active collecting medium in both samplers, and both use colorimetry as the analytical method for detection of NO_2^-. The samplers differ in that the YN device uses TEA-coated on a cellulose filter, with a Teflon® filter as a diffusion barrier; whereas the CH sampler uses TEA-coated on a glass fiber filter, with a polycarbonate filter as a diffusion barrier. Detection limits are reported to be 0.07 ppm·h (Yanagisawa and Nishimura, 1982) and 0.06 ppm·h (Cadoff and Hodgeson, 1983) for the YN and CH samplers, respectively. Interferences from PAN and HNO_2 are expected (Sickles and Michie, 1987); likewise, the devices are sensitive to the speed of ambient air movement.

Palmes tubes have been developed for NO_2 measurement and adapted to NO measurement as described above. The device has been used for workplace and personal exposure monitoring (Wallace and Ott, 1982) and for ambient air measurements (U.S. Environmental Protection Agency, 1993c). A detection limit of 0.03 ppm·h can be achieved if IC is used to determine the extracted NO_2^- (Mulik and Williams, 1986). Adsorption of NO_2 to the tube walls may raise this limit considerably (Miller, 1988), but this effect can be counteracted by use of stainless steel tubes. The device is sensitive to temperature and wind speed, and PAN and HNO_2 are likely interferences (Sickles and Michie, 1987). In a comparison with two commercially produced NO_2 passive samplers, the Palmes tube showed reasonable accuracy and precision at loadings of 1 to 80 ppm·h. However, the commercial devices were designed for use at relatively high loadings; therefore, this comparison does not support the use of Palmes tubes for ambient air monitoring.

3.5.3.4 Calibration Methods

Calibration of NO measurement methods is done using standard cylinders of NO in nitrogen. Typical NO concentrations in such cylinders are 1 to 50 ppmv. Dilution of such standards with clean air using mass flow controllers can accurately provide NO concentrations in the ambient (i.e., 1 to 100 ppbv) range for calibration. Nitric oxide standards are available

as SRMs from NIST and as commercially available Certified Reference Standards. Commercially available certified NO standards have been shown to be stable and accurate for the specified concentrations.

Standard cylinders of NO_2 in nitrogen or air are sometimes used for NO_2 calibration. These standards are commercially available and are readily diluted to parts-per-billion-volume levels in the same manner as for NO standards. However, instability of the NO_2 levels in such standards has been reported, and caution must be used in relying on NO_2 standards as the primary means of calibration.

Two calibration methods for NO_2 are specified in the Code of Federal Regulations (1987) for calibration of ambient NO_2 measurements: (1) permeation tubes and (2) gas-phase titration.

An NO_2 permeation tube is an inert enclosure, generally of Teflon®, glass and Teflon®, or stainless steel and Teflon®, that contains liquid NO_2. As long as liquid NO_2 is present, NO_2 will permeate through the Teflon® at a rate that depends on the temperature of the tube. Maintaining the permeation tube at a constant temperature (i.e., ±0.1 °C) results in permeation of NO_2 at a constant rate. Dilution of the emitted NO_2 with a flow of dry air or N_2 results in known low NO_2 concentrations for calibration. Nitrogen dioxide permeation tubes are supplied as SRMs by NIST, and tubes are commercially available with a wide range of permeation rates. Permeation tubes are small, simple, reliable, and relatively inexpensive, although constant temperature ovens and dilution systems are required to obtain good results. Nitrogen dioxide permeation tubes are susceptible to moisture, and changes in permeation rate or emission of other species (HNO_3, HNO_2, NO) may occur if they are not kept dry. As with NO_2 cylinder standards, the NO_2 permeation tube requires care as a calibration method for NO_2.

Gas-phase titration uses the rapid reaction of NO with O_3 to produce NO_2 with 1:1 stoichiometry. In practice, excess NO generated from a standard cylinder containing 50 to 100 ppmv NO is reacted with O_3 from a stable source. The resultant decrease in NO concentration, usually measured on the NO channel of a CL NO_x analyzer, equals the concentration of NO_2 generated. Varying amounts of NO_2 can be produced by varying the amount of O_3.

3.6 Ozone Air Quality Models

To plan control strategies to achieve compliance with the NAAQS for O_3 at some future date, it is necessary to predict how O_3 concentrations change in response to prescribed changes in source emissions of precursor species (NO_x and VOCs). This assessment requires an air quality model, which in the case of O_3 prediction is often called a photochemical air quality model. The model, in effect, is used to determine the emission reductions needed to achieve the O_3 air quality standard. For at least a decade, EPA has offered guidelines on the selection of air quality modeling techniques for use in SIP revisions, new source reviews, and studies aimed at the prevention of significant deterioration of air quality.

It is worth noting the interrelated nature of O_3 and other air quality issues. Ozone, PM_{10}, visibility, and acid deposition are all connected as a result of similar sources and complex chemical mechanisms. Consequently, strategies for O_3 abatement that involve reductions of VOC and NO_x emissions also will impact particulate matter, visibility, and acid deposition.

Ozone air quality models provide the ability to address "what if" questions, such as, what if emissions of VOCs or NO_x are reduced? The model can be used as an experiment that cannot be run in the atmosphere. Sensitivity questions can be asked, such as, how important is emissions change A relative to emissions change B? or what is the effect of an X% uncertainty in a particular chemical reaction rate constant on the predicted O_3 levels?

Models are the ultimate integrators of our knowledge of the comprehensive chemistry and physics of the atmosphere. As such, they are an indispensable tool for understanding the complex interactions of transport, transformation, and removal in the atmosphere. Models are useful in the design of field measurement programs and are essential in the interpretation of data from such programs.

Models can be verified by the demonstration of agreement between observations and predictions, but confirmation is inherently partial. Verification of mathematical models of natural systems is always incomplete because complete information on the natural system is never available. Furthermore, model results always include some degree of nonuniqueness because model inputs and parameters are never precisely known. Ozone air quality model applications are most reliable in the domain and conditions where model predictions have been evaluated by extensive, valid data and the comparisons of observations and predictions fall within accepted guidelines.

Historically, the primary measure of model performance has been degree of agreement between observed and predicted O_3 concentrations during simulated episodes, although it now is recognized that comparisons of observations and predictions for other compounds, such as organics and NO_y components, are also important in assessing model performance.

The purpose of Section 3.6 is to review briefly the main elements of O_3 air quality models, to describe several of the current models, to discuss the performance evaluation of these models, and to present examples of the use of the models for determining VOC and NO_x control strategies.

3.6.1 Definitions, Description, and Uses

Air quality models are mathematical descriptions of the atmospheric transport, diffusion, removal, and chemical reactions of pollutants. These models operate on sets of input data that characterize the emissions, topography, and meteorology of a region and produce outputs that describe air quality in that region. Mathematical models for photochemical air pollution first were developed in the early 1970s and have been improved, applied, and evaluated since that time. Much of the history of the field is described in reviews by Tesche (1983), Seinfeld (1988), and Roth et al. (1990).

Photochemical air quality models include treatments of the important physical and chemical processes that contribute to O_3 formation in and downwind of urban areas. In particular, such models contain a representation of the following phenomena (Roth et al., 1990):

· Precursor emissions. The spatial and temporal characteristics of reactive hydrocarbon, CO, and NO_x emissions sources must be supplied as inputs to the model. Hydrocarbon emissions generally are apportioned into groups (e.g., alkanes, alkenes, aromatics, etc.) according to the speciation requirements of the chemical kinetic mechanism embedded in the model.

·   Pollutant transport. Once the O_3 precursors are emitted into the atmosphere, they are transported by the wind. When O_3 is formed, it also is subject to transport by the wind. Grid-based models require the preparation of three-dimensional, time-varying fields of wind speed and direction. These values must be specified for each grid cell. Cloud venting and mixing processes that are important on the regional scale also can be included in the pollutant transport description.

·   Turbulent diffusion. Ozone and its precursors also are subject to turbulence-related dispersion processes that take place on a subgrid scale. These turbulent diffusion effects usually are represented in grid-based models by the so-called gradient transport hypothesis, where the pollutant flux is assumed to be proportional to the spatial gradient in the concentration field. The turbulent diffusivities employed in the model are dependent on atmospheric stability and other meteorological variables.

·   Chemical reactions. Ozone results from chemical transformations involving reactive organics and NO_x (See Section 3.2). A chemical kinetics mechanism representing the important reactions that occur in the atmosphere is employed to estimate the net rate of change of each pollutant simulated by the model. Description of chemical reactions requires actinic flux, cloud cover, temperature, and relative humidity.

·   Removal processes. Pollutants are removed from the atmosphere via interactions with surfaces at the ground, so-called "dry deposition", and by precipitation, called "wet deposition".

Guidelines issued by EPA (U.S. Environmental Protection Agency, 1986b) identify two kinds of photochemical model: (1) the grid-based UAM is the recommended model for modeling O_3 over urban areas, and (2) the trajectory model EKMA is identified as an acceptable approach. The 1990 CAAA (U.S. Congress, 1990) mandate that three-dimensional, or grid-based, air quality models, such as UAM, be used in SIPs for O_3 nonattainment areas designated as extreme, severe, serious, or multistate moderate (U.S. Environmental Protection Agency, 1991b).

3.6.1.1 Grid-Based Models

The basis for grid-based air quality models is the atmospheric diffusion equation that expresses the conservation of mass of each pollutant in a turbulent fluid in which chemical reactions occur (Seinfeld, 1986). The region to be modeled is bounded on the bottom by the ground, on the top by some height that characterizes the maximum extent of vertical mixing, and on the sides by east-west and north-south boundaries. The choice of the size of the modeling domain will depend on the spatial extent of the O_3 problem, including the distribution of emissions in the region, the meteorological conditions, and, to some extent, the computational resources available. This space then is subdivided into a three-dimensional array of grid cells. The horizontal dimensions of each cell are usually a few kilometers for urban applications up to tens of kilometers for regional applications. Some older grid-based models assumed only a single, well-mixed vertical cell extending from the ground to the inversion base; current models subdivide the region into layers. Vertical dimensions can vary, depending on the number of vertical layers and the vertical extent of the region being modeled. Increasing the vertical resolution in the computation should be accompanied by increased vertical resolution of the physical parameters used. A compromise generally must

be reached between the better vertical resolution afforded by the use of more vertical layers and the associated increase in computing time. Although aerometric data, such as the vertical temperature profile, which are needed to define the vertical structure of the atmosphere, are generally lacking, it is still important to use enough vertical layers so that vertical transport processes are represented accurately.

There are practical and theoretical limits to the minimum horizontal grid cell size. Increasing the number of cells increases computing and data acquisition effort and costs. In addition, the choice of the dimension of a grid cell implies that the input data information about winds, turbulence, and emissions, for example, are resolved to that scale. The spatial resolution of the concentrations predicted by a grid-based model corresponds to the size of the grid cell. Thus, effects that have spatial scales smaller than those of the grid cell cannot be resolved. Such effects include the depletion of O_3 by reaction with NO near strong sources of NO_x like roadways and power plants. Ozone predictions are sensitive to the choice of grid cell size. The use of a larger grid tends to smooth out VOC and NO_x precursor concentrations, affecting the computed chemical production of O_3. Multigrid models, in which a region with a finer grid resolution is embedded within a larger grid, are an approach to obtain a better resolution of O_3 formation processes in regions of intense source emissions (Odman and Russell, 1991).

Jang (1992) has examined the sensitivity of O_3 predictions to model grid resolution in regional air quality models. A high-resolution version of the Regional Acid Deposition Model (RADM) was used to simulate O_3 formation over the northeastern United States at different grid resolutions. The high-resolution version of RADM, with horizontal grid cell sizes of 20, 40, and 80 km, was operated within the 80-km RADM domain. Coarser grid sizes were found to result in lower resolved emission intensities of NO_x and VOCs. Because of the smearing effect of the large grid sizes, the coarser grid model tended to underpredict the O_3 highs in the areas downwind of cities and overpredict the O_3 lows in the intense NO_x emissions areas. It was found that the impact of model grid resolution on the chemistry of NO_x is more important than that on the chemistry of VOCs, and that model grid resolution has no significant impact on the total amount of odd oxygen ($O_x = O_3 + NO_2$) produced in the models but has great impact on the interactions of chemistry and transport processes that control the balance of O_x. As a result, the coarser grid model tends to predict higher O_3 and lower NO_2 than does the finer grid model, and the coarser grid tends to transport O_x more in the form of O_3, whereas the finer grid model tends to transport the O_x more in the form of NO_2.

Uncertainties arise in photochemical modeling from the basic model components (chemical mechanism and numerical techniques in solving the governing equations) and from inputs to the simulations that reflect the particular episode (boundary and initial conditions, emission inventory, wind field, and mixing depth). Sensitivity studies aim to determine the range of uncertainty in model predictions corresponding to ranges of uncertainty in the basic model components and input quantities. Such studies are valuable in pinpointing those quantities to which model predictions are most sensitive and, therefore, in directing future efforts in reducing the uncertainty in key parameters. These studies are also valuable in assessing the sensitivity of future air quality changes to uncertainties in the base case episode. It is not possible to state general, widely applicable levels of uncertainty for photochemical model inputs and parameters. These will depend on the particular region being modeled, and, in the case of meteorological and emissions inputs, may even depend on the time of day

during the simulation. All model application exercises should include, to the extent possible, an analysis of the uncertainties in model inputs and parameters.

Several grid-based photochemical air quality models have been developed to simulate O_3 production in urban areas or in larger regions. They differ primarily in their treatment of specific atmospheric processes, such as chemistry, and in the numerical procedures used to solve the governing system of equations. These models will be reviewed in Section 3.6.3.

3.6.1.2 Trajectory Models

In the trajectory model approach, a hypothetical air parcel moves through the area of interest along a path calculated from wind trajectories. Emissions are injected into the air parcel and undergo vertical mixing and chemical transformations. The data requirements for trajectory models include: (1) initial concentrations of all relevant pollutants and species; (2) rates of emissions of VOC and NO_x precursors into the parcel along its trajectory; (3) meteorological characteristics, such as wind speed and direction, needed to define the path of the air parcel through the region; (4) mixing depth; and (5) solar ultraviolet radiation.

The key assumption inherent in the trajectory model is that a hypothetical air parcel maintains its integrity along the trajectory. Almost certainly, the parcel assumption fails at night, when flows drift and the atmosphere stratifies; for hilly or mountainous terrain; and under convergence conditions. Thus, the trajectory model concept does not apply in many areas and under a variety of conditions (Liu and Seinfeld, 1975).

Trajectory models provide a dynamic description of atmospheric source-receptor relationships that is simpler and less expensive to derive than that obtained from grid models. Trajectory models are designed to study the photochemical production of O_3 in the presence of sources and vertical diffusion of pollutants; otherwise the meteorological processes are highly simplified.

A simple trajectory model is used in EKMA (Dodge, 1977a). This modeling approach relates the maximum level of O_3 observed downwind of an urban area to the levels of VOCs and NO_x observed in the urban area. It is based on the use of a simple, one-cell moving box model. As the box moves downwind, it encounters emissions of organics and NO_x that are assumed to be uniformly mixed within the box. The height of the box is allowed to expand to account for the breakup of the nocturnal inversion layer. As the height of the box increases, pollutants above the inversion layer are transported into the box. The model is first used to generate a series of constant O_3 lines (or isopleths) as depicted in Figure 3-25. The isopleths show the downwind, peak 1-h O_3 levels as a function of the concentrations of VOCs and NO_x for a hypothetical urban area. These isopleths were generated by carrying out a large number of model simulations in which the initial concentrations and anthropogenic emissions of VOCs and NO_x were varied systematically, whereas all other model inputs were held constant. When it was first conceived, EKMA employed a very simple, highly empirical chemical mechanism and the isopleths generated were for a hypothetical situation in Los Angeles. As understanding of the chemical processes responsible for O_3 formation increased, the EKMA model was updated to include more complete representations of atmospheric chemistry. Although EKMA has employed the CBM-IV mechanism, the same mechanism that is currently being used in several grid-based models, the most recent version allows the input of any mechanism. The EKMA method is
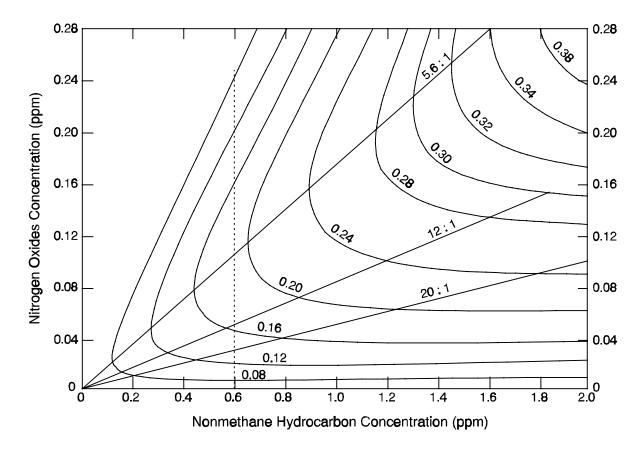
Figure 3-25. Example of Empirical Kinetic Modeling Approach diagram for high-oxidant urban area.

Source: Derived from U.S. Environmental Protection Agency (1986a).

now used to generate city-specific isopleth diagrams using information on emissions, transport, and dilution that are appropriate to the particular city being modeled.

City-specific O_3 isopleths can be used to estimate the reduction in NMHC or NO_x levels needed to achieve the NAAQS for O_3 in a specific urban area. The first step is to determine the early-morning NMHC/NO_x ratio for the urban area in question and the maximum 1-h downwind O_3 concentration. Both the NMHC/NO_x ratio and the peak O_3 concentration are obtained from air monitoring data. These two values define a point on the isopleth surface and, from this point, the percentage reductions in NMHC or NO_x, or both, needed to achieve the O_3 NAAQS can be determined.

As examination of Figure 3-25 reveals, for an NMHC concentration of 0.6 ppmC, for example, increasing NO_x leads to increased O_3 until NMHC/NO_x ratios of about 5:1 to 6:1 are reached; further NO_x increases, leading to lower NMHC/NO_x ratios, inhibit O_3 formation. Thus, in this example, there is a "critical" ratio (in the range of 5:1 to 6:1) at which the NO_x effect on O_3 changes direction. Besides this "critical" ratio, an "equal control" NMHC/NO_x ratio also exists, above which the reduction of NO_x is more beneficial in terms of O_3 reduction than an equal percentage reduction in NMHC. This ratio, for the isopleths

shown in Figure 3-25, is roughly 8:1 to 9:1 for low levels of control and as high as 20:1 for the levels of control needed to reduce O_3 to 0.12 ppm. Thus, for this particular case (Figure 3-25), the chemical mechanism modeling evidence suggests that NO_x control will increase the peak downwind O_3 concentration at $NMHC/NO_x$ ratios of between 5:1 and 6:1 or lower; both NO_x control and NMHC control will be beneficial at somewhat higher ratios, with control of NMHC being more effective; and, for ratios above 20:1, NO_x control is relatively more effective in reducing O_3 to attain the O_3 NAAQS.

The EKMA-based method for determining control strategies has some limitations, the most serious of which is that predicted emissions reductions are critically dependent on the initial $NMHC/NO_x$ ratio used in the calculations. This ratio cannot be determined with any certainty because it is expected to be quite variable in time and space in an urban area. Another limitation is that trajectory models have limited spatial and temporal scopes of application. They are generally 1-day models, simulating only one cell at a time. Another problem with the use of morning $NMHC/NO_x$ ratios is the failure to account for photochemical evolution as urban emissions are carried downwind. As demonstrated in simulations by Milford et al. (1989) and in smog chamber studies by Johnson and Quigley (1989), an urban plume that is in the VOC-controlling regime (low $NMHC/NO_x$ ratio) near city center can move increasingly into the NO_x-controlling regime (high $NMHC/NO_x$ ratio) as the air parcels age and move downwind. This progression occurs because NO_x is photochemically removed from an aging plume more rapidly than VOCs, causing the VOC/NO_x ratio to increase. As demonstrated by Milford et al. (1989), the implication of this evolution is that different locations in a large urban area can show very different O_3 sensitivities to VOC and NO_x changes. Because of this and other drawbacks, the 1990 CAAA (U.S. Congress, 1990) require that grid-based models be used in most O_3 nonattainment areas.

3.6.2 Model Components
3.6.2.1 Emissions Inventory

The spatial and temporal characteristics of VOC and NO_x emissions must be supplied as inputs to a photochemical air quality model. Emissions from area and point sources are injected into ground-level grid cells, and emissions from large point sources are injected into upper level cells. Total VOC emissions generally are apportioned into groups of chemically similar species (e.g., alkanes, alkenes, aromatics, etc.) according to the requirements of the chemical mechanism. This apportionment may be accomplished using actual emission sampling and analysis or be based on studies of similar emission sources. Recognition of potential undercounting in existing inventories has spurred efforts to improve the accuracy of emissions inventories. In fact, at present, the emissions inventory is the most rapidly changing component of photochemical models. It has been recognized that both mobile and stationary source components have been highly uncertain and that there is significant ongoing effort to improve the accuracy of emissions inventories.

Some emissions terminology is as follows (Tesche, 1992):
- Emissions data—the primary information used as input to emissions models.
- Emissions model—the integrated collection of calculational procedures, or algorithms, properly encoded for computer-based computation.
- Emissions estimates—the output of emissions models; used as input to photochemical models.

- Emissions inventory—the aggregated set of emissions estimate files.
- Emissions model evaluation—the testing of a model's ability to produce accurate emissions estimates over a range of source activity and physicochemical and meteorological conditions.

Emissions input requirements for the UAM, for example, include:
- Spatial allocation of precursor emissions (VOCs, NO_x, CO):
  — Actual location of individual point sources;
  — Spatial allocation by gridding surrogates;
  — Assignment of surrogates to other categories.
- Stack parameters for point sources:
  — Temperature, height, diameter, and exit velocity.
- Speciation of VOC emissions for CBM-IV mechanism:
  — Region-specific speciation profiles;
  — EPA default speciation profiles.
- Temporal allocation of precursor emissions:
  — Operating schedules for individual point sources;
  — Assignment of diurnal profiles for area and mobile sources.

The emissions inventory component of modeling is moving in the direction of the use of emissions models rather than inventories. Emissions models are being developed for the Lake Michigan Oxidant Study (LMOS), the San Joaquin Valley Air Quality Study (SJVAQS), and the Atmospheric Utility Signatures, Predictions, and Experiments (AUSPEX), designated as the SJVAQS/AUSPEX Regional Model Adaptation Project (SARMAP). The consistency of existing inventories was improved in 1990 when EPA released the Emissions Preprocessor System (EPS) as a component of the UAM (U.S. Environmental Protection Agency, 1992b). The EPS was updated in 1992 to EPS Version 2 (EPS2). It is an emissions model that considers spatial and temporal disaggregation factors, speciation data, and meteorological data to convert daily emissions estimates for each point source and for area source categories and mobile source emissions factors computed by the EPA MOBILE5 model into hourly, gridded speciated estimates that are needed by a photochemical grid model.

A step beyond the EPS is the Emissions Modeling System (EMS)[1] (Tesche, 1992). The EMS utilizes emissions estimation and information processing methods to provide gridded, temporally resolved, and chemically speciated base-year emissions estimates for all relevant source categories; to provide flexibility in forecasts of future-year emissions rates; and to provide modular code design for use in module updating and replacement. The EMS provides for easy substitution of alternative assumptions, theories, or input parameters (e.g., emissions factors, activity levels, spatial distributions) and facilitates sensitivity and uncertainty testing.

As a result of a variety of independent studies, it recently has been determined that urban VOC emissions inventories, particularly motor vehicle emissions, have been significantly understated. These studies include tunnel studies (Pierson et al., 1990) and comparisons of ambient and emission inventory VOC/NO_x ratios (Fujita et al., 1992).

---

[1]The EMS has been renamed the GMEP (Geocoded Model of Emissions and Projections).

3.6.2.2 Meteorological Input to Air Quality Models

Grid-based air quality models require, as input, the three-dimensional wind field for the episode being simulated. This input is supplied by a so-called meteorological module. Meteorological modules for constructing wind fields for air quality models fall into one of four categories (Tesche, 1987; Kessler, 1988):

(1) Objective analysis procedures that interpolate observed surface and aloft wind speed and direction data throughout the modeling domain;

(2) Diagnostic methods in which the mass continuity equation is solved to determine the wind field;

(3) Dynamic, or prognostic, methods based on numerical solution of the governing equations for mass, momentum, energy, and moisture conservation, along with the thermodynamic state equations on a three-dimensional, finite-difference mesh; or

(4) Hybrid methods that embody elements from both diagnostic and prognostic approaches.

Objective Analysis

Objective wind-field analysis involves the interpolation and extrapolation of wind speed and direction measurements (collected at a number of unequally spaced monitoring stations) to grid points throughout the region (Goodin et al., 1980). For flat terrain settings away from complex mesoscale forcings, this class of techniques may provide an adequate method for estimating the wind field, provided that appropriate weighting and smoothing functions are used (Haltiner, 1971). For complex terrain or coastal/lake environments, however, it is tenuous to interpolate between and extrapolate from surface observational sites except with an unusually dense monitoring network. In most cases, the routinely available rawinsonde network sounding data are even more severely limited because of the large distances (300 to 500 km) between sites and because soundings are made only every 12 h. The limitations of even the best available data sets are most severe above the surface layer, where upper level observations are less frequent and more expensive to obtain. It will remain economically unfeasible to obtain sufficiently dense atmospheric observations to allow any direct objective analysis scheme to provide the required detail and accuracy necessary for use in advanced, high-resolution photochemical models.

Diagnostic Modeling

In diagnostic wind modeling, the kinematic details of the flow are estimated by solving the mass conservation equation. Dynamic interactions such as turbulence production and dissipation and the effects of pressure gradients are parameterized. Various diagnostic wind models have been developed, many employing the concepts introduced by Sherman (1978) and Yocke (1981).

In recent years, attempts have been made to combine the best features of objective analysis and pure diagnostic wind modeling. The current release of EPA's UAM-IV includes the Diagnostic Wind Model (DWM) as the suggested wind-field generator for this urban-scale photochemical model. The DWM (U.S. Environmental Protection Agency, 1990c) is representative of this class of hybrid objective-diagnostic models. The DWM combines the features of the Complex Terrain Wind Model (CTWM) (Yocke, 1981) and the objective wind interpolation code developed at the California Institute of Technology (Goodin et al., 1980). In the DWM, a two-step procedure normally is followed. First, a "domain-scale" wind is

estimated from available surface and upper-air synoptic data. This initial field consists of a single wind vector (e.g., horizontal homogeneity) for each elevation. The domain-scale wind is adjusted using procedures derived from the CTWM for the kinematic effects of terrain such as lifting, blocking, and flow acceleration. Thermodynamically generated influences such as mountain-valley winds are parameterized. This first step produces a horizontally varying field of wind speed and direction for each vertical layer within the DWM modeling domain. Typically, 10 to 12 vertical layers are used. In the second step, available hourly surface and upper air measurements are combined objectively with the step 1 hourly diagnostic flow fields to produce a resultant wind field that matches the observations at the monitoring points and obeys the general constraints of topography in regions where data are absent. The DWM contains a number of user-specified options whereby different final flow fields may be produced, depending on selection of various smoothing and weighting parameters. The final output of the DWM is a set of hourly averaged horizontal wind fields for each model layer.

Diagnostic models may invoke scaling algorithms that propagate the influence of the surface-flow field into upper levels according to the local height of the inversion and the Pasquill-Gifford-Turner stability category for the hour. Once the winds are created by DWM, they must be "mapped" onto the photochemical model's vertical grid structure. This function is normally accomplished in a two-step process. First, the DWM winds are interpolated onto the photochemical model grid using simple linear interpolation. Second, the three-dimensional divergence is computed in each grid cell and an iterative scheme is used to minimize this divergence to a user-specified level. Typically, the output consists of "nondivergent" x- and y-direction wind components for direct input to the photochemical model.

Among the advantages of the diagnostic modeling approach are its intuitive appeal and modest computing requirements. The method generally reproduces the observed wind values at the monitoring locations and provides some information on terrain-induced airflows in regions where local observations are absent. In addition, diagnostic model parameters for a particular locale based on site-specific field measurements may be calibrated. However, there are several disadvantages. Diagnostic models cannot represent complex mesoscale circulations, unless these features are well represented by surface and aloft observations. Often the vertical velocities produced by a diagnostic model are unrealistic and, in regions of complex terrain, local horizontal flow velocities often may be an order of magnitude too high (Tesche et al., 1987). Because the diagnostic model is not time-dependent, there is no inherent dynamic consistency in the winds from one hour to the next. That is, calculation of the flow field at 1200 hours, for example, is not influenced by the results of the 1100-hour winds. This is a particular problem in applications involving important flow regimes, such as land-sea breezes, mountain-valley winds, eddy circulations, and nocturnal valley jets, that take several hours to develop and whose three-dimensional character is poorly characterized by even the most intensive sampling networks. Finally, the inadequacy of the upper-air synoptic data causes significant difficulty in the validation of the model wind fields.

Prognostic Modeling

In prognostic meteorological modeling, atmospheric fields are computed based on numerical solutions of the coupled, nonlinear conservation equations of mass, momentum, energy, and moisture. Derivations of these equations are presented extensively in the literature (Haltiner, 1971; Pielke, 1984; Seinfeld, 1986; Cotton and Anthes, 1989). Many prognostic models have been developed for computing mesoscale wind fields, as shown in the

recent survey by Pielke (1989), and they have been applied to a variety of problems, including the study of land-sea and land-lake circulations. Available prognostic models range from relatively simple one-dimensional representations to complex three-dimensional codes.

Prognostic wind models are attractive because they explicitly address the various physical processes governing atmospheric flows. Consequently, they have the potential for describing a number of wind regimes that are particularly relevant to air pollution modeling, such as flow reversal, daytime upslope flows, wind shear, and other mesoscale thermally induced circulations. Drawbacks of prognostic models include the need to gather detailed data for model performance testing and the large computational costs. Indeed, prognostic models may require as much or more computer time than regional-scale photochemical models. More intensive data sets are needed to evaluate prognostic models than for diagnostic models, but this is not necessarily a disadvantage. Rather, it provides the modeler and decision-maker with a far better basis for judging the adequacy of the model than can be achieved with objective or diagnostic models.

Summaries of prognostic models available for use in air quality modeling are presented extensively in the literature (e.g., Pielke, 1989; Benjamin and Seaman, 1985; McNally, 1990; Stauffer et al., 1985; Stauffer and Seaman, 1990; Ulrickson, 1988; Wang and Warner, 1988; and Yamada et al., 1989). From these reviews, two models stand out as representing the present state-of-science in applications-oriented prognostic modeling. These are the Mesoscale Model Versions 4 and 5 (MM4/MM5) developed by Pennsylvania State University and the National Center for Atmospheric Research (NCAR) (Anthes and Warner, 1978; Anthes et al., 1987; Zhang et al., 1986; Seaman, 1990; Stauffer and Seaman, 1990), and the Coast and Lake Regional Atmospheric Modeling System (CAL-RAMS) (Tripoli and Cotton, 1982; Pielke, 1974, 1984, 1989; Lyons et al., 1991).

Three ongoing regional O_3 modeling programs in the United States are using prognostic models to drive regional O_3 models. These include LMOS; SARMAP; and a regional O_3 modeling program in Southeast Michigan, Northern Ohio, and Southwest Ontario. Part of EPA's long-range plan (in the Office of Research and Development [ORD]) for model development is to construct a "third" generation modeling framework referred to as MODELS 3 (Dennis and Novak, 1992). This modeling system will consolidate all of the agency's three-dimensional models. The current plan calls for meteorological inputs to the MODELS 3 system to be supplied by prognostic models. The MM4 model (the hydrostatic version of MM5) is presently being examined by EPA for this purpose.

Activities are currently underway in LMOS to supply prognostic model fields to EPA's ROM for use in simulating regional O_3 distributions in four multiple-day O_3 episodes extensively monitored during the 1991 field program in the midwest. The EPA will be utilizing ROM2.2 (version 2.2) with fields obtained from CAL-RAMS (Lyons et al., 1991) to examine whether prognostic model output gives improved regional O_3 estimates (Guinnup and Possiel, 1991).

The SARMAP program is the modeling and data analysis component of a multiyear collaboration between two projects, SJVAQS and AUSPEX. The major near-term objective of SARMAP is to understand the processes that lead to high O_3 concentrations in the San Joaquin Valley of California. An overview of the regional meteorological and air quality modeling approach of SARMAP is described by Tesche (1993). For SARMAP, the MM5 model was chosen as the "platform" prognostic meteorological model because of its broad application history; its demonstrated reliability on large domains, requiring spatially and temporally varying boundary conditions; and its capability for four-dimensional data

assimilation (FDDA)—needed for longer-range simulations (see Section 3.6.2.2). All of these attributes are crucial to the success of mesoscale meteorological modeling.

Prognostic models are believed to provide a dynamically consistent, physically realistic, three-dimensional representation of the wind and other meteorological variables at scales of motion not resolvable by available observations. However, the meteorological fields generated by a prognostic model do not always agree with observational data. Numerical approximations, physical parameterizations, and initialization problems are among the potential sources of error growth in model forecasts that can cause model solutions to deviate from actual atmospheric behavior. Methods that have been devised over the past 20 years to mitigate these problems are described below.

"Post-processing" refers to methods whereby output fields from prognostic models are selectively adjusted through a series of objective techniques with the aim of improving the realism of the resultant fields. Examples of this procedure (sometimes referred to as objective combination) are given by Cassmassi et al. (1991) in the Los Angeles Basin, Kessler and Douglas (1989) in the South Central Coast Air Basin, and Moore et al. (1987) in the San Joaquin Valley.

Ideally, a prognostic model should be initialized with spatially varying, three-dimensional fields (i.e., wind, temperature, moisture) that represent the state of the atmosphere at the initial simulation time. A prognostic model that is initialized with such fields, however, can generate large nonmeteorological "waves" when the initial conditions do not contain a dynamic balance consistent with the model formulation (Hoke and Anthes, 1976; Errico and Bates, 1988). The objective of an initialization procedure is to bring the initial conditions into dynamic balance so that the model can integrate forward with a minimum of noise and a maximum of accuracy (Haltiner and Williams, 1980). Dynamic initialization makes use of a model's inherent adjustment mechanism to bring the wind and temperature into balance prior to the initial simulation time. In this technique, a "presimulation" integration of the model equations produces a set of dynamically balanced initial conditions. By allowing the simulation to begin with a balanced initial state, this technique reduces the generation of meteorological noise and thus improves the quality of the simulation.

Four-Dimensional Data-Assimilation Techniques

Four-dimensional data assimilation refers to a class of procedures in which observational data are used to enhance the quality of meteorological model predictions (Harms et al., 1992). The most common use of FDDA today in applications-oriented models is known as Newtonian relaxation, or simply as "nudging". With this method, model estimates at a particular time interval are adjusted toward the observations by adding artificial tendency terms to the governing prognostic equations. The objective of this method is to improve prognostic model estimates through the use of valid, representative observational data. As an example of this procedure, a linear term is added to the momentum equations to "nudge" the dynamic calculation towards the observed state at each time step in regions where data are available. The FDDA procedures may be thought of as the joint use of a dynamic meteorological model in conjunction with observed data (or analysis fields based on these data) in such a manner that the prognostic equations provide temporal continuity and dynamic coupling of the hourly fields of monitored data (Seaman, 1990).

A recent example of the use of FDDA in regional-scale applications with the MM4/RADM model is given by Stauffer and Seaman (1990). Attempts to apply FDDA in

support of urban-scale photochemical grid modeling are described by Tesche et al. (1990b) and McNally (1990) for the San Diego Air Basin and by Stauffer et al. (1993) for the Grand Canyon region of Arizona. Currently, FDDA is being used in the CAL-RAMS simulations in the LMOS program (Lyons et al., 1991) and in the MM5 simulations for SARMAP (Seaman, 1992).

3.6.2.3 Chemical Mechanisms

A chemical kinetic mechanism (a set of chemical reactions), representing the important reactions that occur in the atmosphere, is used in an air quality model to estimate the net rate of formation of each pollutant simulated as a function of time.

Various grid models employ different chemical mechanisms. Because so many VOCs participate in atmospheric chemical reactions, chemical mechanisms that explicitly treat each individual VOC component are too lengthy to be incorporated into three-dimensional atmospheric models. "Lumped" mechanisms are therefore used (e.g., Lurmann et al., 1986; Gery et al., 1989; Carter, 1990; Stockwell et al., 1990). These lumped mechanisms are highly condensed and do not have the ability to follow explicit chemistry because of this lumping. Lumped-molecule mechanisms group VOCs by chemical classes (alkanes, alkenes, aromatics, etc.). Lumped-structure mechanisms group VOCs according to carbon structures within molecules. In both cases, either a generalized (hypothetical) or surrogate (actual) species represents all species within a class. Organic product and radical chemistry is limited to a few generic compounds to represent all products; thus, chemistry after the first oxidation step is overly uniform. Some mechanisms do not conserve carbon and nitrogen mass. Some molecules do not easily "fit" the classes used in the reduced mechanisms. Because different chemical mechanisms follow different approaches to lumping, and because the developers of the mechanisms made different assumptions about how to represent chemical processes that are not well understood, models can produce somewhat different results under similar conditions (Dodge, 1989).

No single chemical mechanism is currently considered "best". Both UAM-IV and ROM utilize the carbon-bond mechanism (CBM-IV), which, along with the SAPRC (Statewide Air Pollution Research Center, University of California, Riverside) and RADM mechanisms, is considered to represent the state of the science (Tesche et al., 1993; National Research Council, 1991). Agreement among mechanisms is better for O_3 than for other secondary pollutants (Dodge, 1989, 1990; National Research Council, 1991), raising concern that the mechanisms may suffer from compensating errors. These mechanisms are at least 5 years old and often are tested on much older smog chamber data.

The chemical mechanisms used in existing photochemical O_3 models contain uncertainties that may limit the accuracy of the model predictions. The reactions that are included in these mechanisms generally fall into one of three categories.

(1) Reactions for which the magnitude of their rate constants and their product distribution is well known. These include mostly the inorganic reactions and those for the simple carbonyls.

(2) Reactions with known rate constants and known products but with uncertain product yields. These are mostly organic reactions, and the actual product yields assumed may vary among mechanisms.

(3) Reactions with known rate constants but unknown products. Each mechanism assumes its own set of products for reactions in this class. This class includes aromatic oxidation reactions.

Most inorganic gas-phase processes are understood. Regarding classes of VOCs the following general comments can be made:

- The *n*-alkanes comprise approximately one-half of the major carbon emissions in urban areas. Reaction rates are relatively slow. The only important reaction is with the hydroxyl radical. For alkanes C_4 or below, the chemistry is well understood and the reaction rates are slow. For C_5 and higher alkanes the situation is more complex because few reaction products have been found.
- Branched-chain alkanes have rates of reaction that are highly dependent on structure. Rate constants have been measured for only a few of the branched alkanes, and reaction products for this class of organics are not well characterized.
- Alkenes are reactive with OH, O_3, and the NO_3 radical. Most rate constants of these reactions are known. Alkenes make up $\leq 15\%$ of the emitted carbon and constitute about 25% of the hydrocarbon reactions in urban areas. Ozone reaction products are not well characterized, and the mechanisms are poorly understood. Mechanisms for the NO_3 radical are also uncertain.
- Aromatics constitute about 15 to 20% of the carbon compounds emitted and 25% of the hydrocarbons reacting in urban areas. Aromatics have been studied frequently, but only a few reaction products have been well characterized. Aromatics act as strong NO_x sinks under low NO_x conditions.

Mechanisms used in photochemical air quality models thus have uncertainties, largely attributable to a lack of fundamental data on products and product yields. The missing information necessitates that assumptions be made. Current mechanisms provide acceptable overall simulation of O_3 generation in smog chamber experiments. Specific VOCs may, however, be simulated poorly, and products other than O_3 may not be simulated accurately. Existing mechanisms are mostly applicable to single-day, high NO_x conditions because those are the conditions of almost all smog chamber experiments. Low NO_x condition simulations are verified less thoroughly. Fundamental kinetic data are needed on the photooxidation of aromatics, higher alkanes, and higher alkenes to fill in areas of uncertainty in current mechanisms. Whereas these uncertainties are important and require continued research to remove, the uncertainties are likely not such that general conclusions about the relative roles of hydrocarbons and NO_x in O_3 formation will be changed by new data.

3.6.2.4 Deposition Processes

Species are removed from the atmosphere by interaction with ground-level surfaces, so-called dry deposition, and by absorption into airborne water droplets followed by transport of the water droplets, wet deposition. Dry deposition is an important removal process for ozone and other species on both the urban and regional scales and is included in all urban and regional scale models as a contribution to the ground-level flux of pollutants. Wet deposition is a key removal process for gaseous species on the regional scale and is included in regional scale acid deposition models. Urban-scale photochemical models generally have not included a treatment of wet deposition as O_3 episodes do not occur during periods of significant clouds or rain.

Dry Deposition

It is generally impractical to simulate, in explicit detail, the complex of multiple physical and chemical pathways that result in dry deposition to individual surface elements. Because of this, the usual practice has been to adopt simple parameterizations that consolidate the multitude of complex processes. For example, it generally is assumed that the dry deposition flux is proportional to the local pollutant concentration [at a known reference height (z_r), typically 10 m], resulting in the expression $F = -v_d C$, where F represents the dry deposition flux (the amount of pollutant depositing to a unit surface area per unit time), and C is the local pollutant concentration at the reference height. The proportionality constant, v_d, has units of length per unit time and is known as the deposition velocity.

It is customary to interpret the dry deposition process in terms of the electrical resistance analogy, where transport of material to the surface is assumed to be governed by three resistances in series: (1) the aerodynamic resistance (r_a), (2) the quasi-laminar layer resistance (r_b), and (3) the surface or canopy resistance (r_s) (Wu et al., 1992). The aerodynamic resistance characterizes the turbulent transport through the atmosphere from reference height z_r down to a thin layer of stagnant air very near the surface. The molecular-scale diffusive transport across the thin quasi-laminar sublayer near the surface is characterized by r_b. The chemical interaction between the surface and the pollutant of interest once the gas molecules have reached the surface is characterized by r_c. The total resistance (r_t) is the sum of the three individual resistances, and is, by definition, the inverse of the deposition velocity, $1/v_d = r_t = r_a + r_b + r_s$. Note that the deposition velocity is small when any one of the resistances is large. Hence, either meteorological factors or the chemical interactions on the surface can govern the rate of dry deposition.

Dry deposition velocities of HNO_3 and SO_2 are typically ≈ 2 cm s^{-1}, and those of O_3 and PAN are generally ≈ 0.5 and ≈ 1 cm s^{-1}, respectively (Dolske and Gatz, 1985; Colbeck and Harrison, 1985; Huebert and Robert, 1985; Shepson et al., 1992). With a 1 km-deep inversion or boundary layer, the time scale for dry deposition is on the order of 1 day for a deposition velocity of 1 cm s^{-1}. Dry deposition is important for those chemicals with high or fairly high deposition velocities and long or fairly long lifetimes (≥ 10 days) due to photolysis and chemical reaction (for example, HNO_3, SO_2, and H_2O_2, as well as O_3 and PAN).

A number of researchers have reviewed the deposition literature and provided summaries of deposition velocity data. The rank ordering of deposition velocity values among pollutant species based on several such studies is summarized as follows:

McRae and Russell (1984):
$HNO_3 > SO_2 > NO_2 \approx O_3 > PAN > NO$;
Derwent and Hov (1988):
$HNO_3 > SO_2 = O_3 > NO_2 > PAN$;
McRae et al. (1982b):
$O_3 > NO_2 > PAN > NO > CO$; and
Chang et al. (1987):
$HNO_3 > H_2O_2 > NH_3 > HCHO > O_3 = SO_2 = NO_2 = NO > RCHO$.

There is general agreement that HNO_3 is removed at the highest observed rates, which is consistent with the relative deposition rates observed by Huebert and Robert (1985). Most of the surveys are roughly consistent with the relative deposition velocity ordering seen in the experiments of Hill and Chamberlain (1976): diffusion-limited acids > SO_2 > NO_2 $\approx$ O_3 > PAN > NO > CO. This suggests surface resistance values should be ordered approximately as CO > NO > PAN > O_3 $\approx$ NO_2 > SO_2 > HNO_3 = 0. However, there is still a substantial range of variability in reported deposition velocities. For example, McKeen et al.

(1991) calculated dry deposition velocities for HNO_3, O_3, and PAN of 10, 0.5, and 0.3 cm s^{-1}, respectively. Note that a large deposition velocity for HNO_3 will limit the lifetime of HNO_3 relative to O_3 in photochemically aged air.

There are a significant number of other gases for which there are no surface resistance data and for which values must be estimated using expert judgment. The values should be consistent with the existing experimental values for vegetative surfaces and should preserve the apparent rank ordering among the pollutant species (discussed above). For O_3, surface resistance values by land-use type and season recommended by Sheih et al. (1986) and Wesely (1988) are appropriate. For NO, NO_2, NH_3, H_2O_2, HCHO, and CH_3CHO, the surface resistance values for each land use can be estimated from that for SO_2 (Wesely, 1988), except different proportionality factors should be used for NO and NO_2.

The treatment of dry deposition is perhaps the most primitive of the scientific modules in photochemical air quality models. Knowledge of deposition rates is limited, and uncertainties in deposition velocities are high. For travel times of one to several days, the quantities of pollutants that are predicted to be removed by dry deposition can be substantial for those species with appreciable deposition velocities. Setting all species deposition velocities to zero in a model provides an indication of the importance of dry deposition relative to other processes influencing pollutant dynamics. Further effort to describe the dynamics of deposition are needed, together with evaluation against available data that can be used to test deposition modules.

Wet Deposition

Wet deposition refers to the removal of gases and particles from the atmosphere by precipitation events, through incorporation of gases and particles into rain, cloud, and fog water followed by precipitation at the earth's surface. Removal of gases and particles during snow falls is also wet deposition. Wet removal of gases arises from equilibrium partitioning of the chemical between the gas and aqueous phases (Bidleman, 1988; Mackay, 1991). This partitioning can be defined by means of a washout ratio, Wg, with Wg = [C]rain/[C]air, where [C]rain and [C]air are the concentrations of the chemical in the aqueous and gas phases, respectively. Because Wg is the inverse of the air/water partition coefficient, K_{aw}, then Wg = RT/H, where R is the gas constant, T is the temperature, and H is the Henry's Law constant (Mackay, 1991).

Particles and particle-associated chemicals are efficiently removed from the atmosphere by precipitation events, and the washout ratios for particles, Wp, are typically in the range 10^4 to 10^6 (Eisenreich et al., 1981; Bidleman, 1988). Wet deposition is important for particles (and particle-associated chemicals) and for those gas-phase compounds with washout ratios of Wg $\geq 10^4$. Examples of such gaseous chemicals are HNO_3, H_2O_2, phenol, and cresols, all of which are highly soluble in water. Formaldehyde is present in the aqueous phase as the glycol, $H_2C(OH)_2$, and has an effective washout ratio of 7×10^3 at 298 K (Betterton and Hoffmann, 1988; Zhou and Mopper, 1990). Note that the importance of wet deposition may depend on whether the chemical is present in the gas phase or is particle-associated. For example, the gas-phase alkanes have low values of Wg and are inefficiently removed by wet deposition, whereas the particle-associated alkanes are efficiently removed by wet deposition (Bidleman, 1988), through removal of the host particles.

3.6.2.5 Boundary and Initial Conditions

When a grid-based photochemical model is applied to simulate a past pollution episode, it is necessary to specify the concentration fields of all the species computed by the model at the beginning of the simulation. These concentration fields are called the initial conditions. Throughout the simulation, it is necessary to specify the species concentrations, called the boundary conditions, in the air entering the three-dimensional geographic domain.

Three general approaches for specifying boundary conditions for urban-scale applications can be identified: (1) use the output from a regional-scale photochemical model, (2) use objective or interpolative techniques with ambient observational data, or (3) use default regional background values and expand the area that is modeled for urban areas sufficiently isolated from significant upwind sources.

In the ideal case, observed data would provide information about the concentrations for all the predicted species at the model's boundaries. An alternative approach is to use regional models to set boundary and initial conditions. This is, in fact, preferred when changes in these conditions are to be forecast. In any event, simulation studies should use boundaries that are far enough from the major source areas of the region that concentrations approaching regional values can be used for the upwind boundary conditions. Boundary conditions at the top of the area that is being modeled should use measurements taken from aloft whenever they are available. Regional background values often are used in lieu of measurements. An emerging technique for specifying boundary conditions is the use of a nested grid, in which concentrations from a larger, coarse grid are used as boundary conditions for a smaller, nested grid with finer resolution. This technique reduces computational requirements compared to those of a single-size, fine-resolution grid.

Initial conditions are determined mainly with ambient measurements, either from routinely collected data or from special studies. Where spatial coverage with data is sparse, interpolation can be used to distribute the surface ambient measurements. Because few measurements of air quality data are made aloft, it generally is assumed that species concentrations are initially uniform in the mixed layer and above it. To ensure that the initial conditions do not dominate the performance statistics, model performance should not be assessed until the effects of the initial conditions have been swept out of the grid.

3.6.2.6 Numerical Methods

The core of a grid-based O_3 air quality model is the numerical solution of the three-dimensional atmospheric diffusion equation (McRae et al., 1982c). The central numerical schemes involve horizontal advection and simultaneous vertical mixing, advection, and chemistry. A possible source of model inaccuracy is the numerical method used to solve the governing equations. The solution of chemical kinetics is generally the most computationally intensive step in O_3 air quality models. To compute the rate of chemical reaction one essentially must solve a system of stiff nonlinear ordinary differential equations. The desirable characteristics of the integration routine are speed and stability, at a certain prescribed level of accuracy. The chemistry integration routines used in several ozone air quality models are based on the implicit, hybrid, exponential scheme developed by Young and Boris (1977). The integration is stable, efficient, and sufficiently accurate. It has been concluded from several studies that the numerical solution of the vertical/chemical portion of the model is less likely to be a source of O_3 prediction inaccuracy (Odman et al., 1992) than the horizontal advection, numerical method (McRae et al., 1982; Chock, 1985, 1991; Dabdub and Seinfeld, 1994). Although the horizontal transport computations typically consume only a small fraction of the total computer time, it is well known that numerical diffusion and

dispersion degrade the computed solution and that available methods differ greatly in their numerical performance in this regard (Chock, 1985, 1991; Dabdub and Seinfeld, 1994). Continued work on optimizing the numerical methods used in O_3 air quality models is necessary.

3.6.3 Urban and Regional Ozone Air Quality Models

Several grid-based models have been widely used to evaluate O_3 and acid deposition control strategies.

- The Urban Airshed Model, developed by Systems Applications, Inc., has been, and continues to be, applied to urban areas throughout the country. It is described in Section 3.6.3.1. The current EPA-approved version is UAM-IV. The UAM-V, which has been developed for LMOS, is a nested regional-scale model.
- The California Institute of Technology (CIT) model has been applied to California's South Coast Air Basin (McRae et al., 1982a,b; McRae and Seinfeld, 1983; Milford et al., 1989; Harley et al., 1993).
- The ROM, developed by EPA, has been applied to the northeastern and southeastern United States (Schere and Wayland, 1989a,b). It is described in Section 3.6.3.2.
- The Acid Deposition and Oxidant Model (ADOM) was developed by ENSR Consulting and Engineering for the Ontario Ministry of the Environment and Environment Canada (Venkatram et al., 1988) and the German Umweltbundesamt. Its primary application has been to acidic deposition.
- The RADM was developed by NCAR and the State University of New York for NAPAP. The primary objective of RADM applications is the calculation of changes in sulfur and nitrogen deposition over the eastern United States and southeastern Canada, resulting from changes in emissions (National Acid Precipitation Assessment Program, 1989). See Section 3.6.3.3 for a description of RADM.

A summary of the major applications of the above air quality models, including the Sulfur Transport Eulerian Model (STEM-II), is presented in Table 3-21. All of the models are based nominally on a 1-h time resolution. The horizontal spatial resolutions vary from 5 to 120 km. Typical spatial resolutions used in past model applications are summarized in Table 3-22. It is important to note that the spatial scale at which a model is applied is governed by the manner in which physical processes are treated and the spatial scale of the inputs. The regional models can have a vertical resolution on the order of 10 to 15 layers extending up to 6 to 10 km in order to treat vertical redistribution of species above the planetary boundary layer. This increased vertical resolution often comes at the expense of decreased horizontal resolution. Urban models typically have two to five layers extending up to 1,000 to 2,000 m. The treatment of meteorological fields by the six models is summarized in Table 3-23. Generally, the treatment of meteorology is separate from the air quality model itself, and models can employ wind fields prepared by different approaches as long as consistent assumptions, such as nondivergent wind field, are employed in each model. The regional models, ROM, RADM, ADOM, and STEM-II, address the vertical redistribution of pollutants resulting from the presence of cumulus clouds.

Table 3-21. Grid-Based Urban and Regional Air Pollution Models:
Overview of Three-Dimensional Air Quality Models[a]

Model	Major Applications	Major References for Model Formulation	Selected References for Model Performance Evaluation and Application
UAM	Urban and nonurban areas in the United States and Europe	Reynolds et al. (1973, 1974, 1979) Tesche et al. (1992) U.S. Environmental Protection Agency (1990a,b,c; 1992b) Scheffe and Morris (1993)	Tesche et al. (1993)
CIT	Los Angeles Basin	McRae et al. (1982a)	McRae and Seinfeld (1983) Russell et al. (1988a,b) Harley et al. (1993)
ROM	Eastern United States (E of 99° W longitude)	Lamb (1983)	Schere and Wayland (1989a,b) Meyer et al. (1991b)
RADM	Eastern North America	Chang et al. (1987)	Middleton et al. (1988, 1993) Middleton and Chang (1990) Dennis et al. (1993a) Cohn and Dennis (1994)
ADOM	Eastern North America and Northern Europe	Venkatram et al. (1988)	Venkatram et al. (1988) Macdonald et al. (1993) Karamchandani and Venkatram (1992)
STEM-II	Philadelphia area, Kentucky, and northeastern United States, central Japan	Carmichael et al. (1986)	Carmichael et al. (1991) Saylor et al. (1991)

[a]See Appendix A for abbreviations and acronyms.

Table 3-22. Grid-based Urban and Regional Air Pollution Models: Treatment of Emissions and Spatial Resolution[a]

Model	Emitted Species	Point-Source Emissions	Area-Source Emissions	Vertical Resolution
UAM	SO_2, sulfate, NO, NO_2, CO, NH_3, and 8 classes of ROG and PM (4 size classes)	Released into grid cell in layer corresponding to plume rise in UAM; treated with a reactive plume model in PARIS	Grid-average with resolution ranging from 4 km × 4 km to 10 km × 10 km in past applications	Typically, 5-6 layers up to about 1.5 km
CIT	SO_2, sulfate, NO, NO_2, CO, NH_3, and 6 classes of ROG and PM (4 size classes)	Treated with a plume model with simple NO_x and O_3 chemistry	Grid-average with 5 km × 5 km resolution in past applications	Five layers up to about 1.5 km
ROM	CO, NO, NO_2, and 8 classes of ROG	Released into grid cell in layer corresponding to plume rise	Grid-average with 18.5 km × 18.5 km resolution in present applications	Three layers up to about 4 km
RADM	SO_2, sulfate, NO, NO_2, CO, NH_3, and 12 classes of ROG	Released into grid cell in layer corresponding to plume rise	Grid-average with 80 km × 80 km resolution in past applications	Fifteen layers up to about 16 km
ADOM	SO_2, sulfate, NO, NO_2, NH_3, and 8 classes of ROG and PM	Released into grid cell in layer corresponding to plume rise	Grid-average with resolution ranging from 60 km × 60 km to about 120 km × 120 km in past applications	Twelve layers up to about 10 km
STEM-II	SO_2, sulfate, NO, NO_2, NH_3, and 8 classes of ROG	Released into grid cell in layer corresponding to plume rise	Grid-average with resolution ranging from 10 km × 10 km to 56 km × 56 km in past applications	Ten to 14 layers up to about 6 km

[a]See Appendix A for abbreviations and acronyms.

**Table 3-23. Grid-based Urban and Regional Air Pollution Models:
Treatment of Meteorological Fields, Transport, and Dispersion[a]**

Model	Meteorology	Transport	Turbulent Diffusion
UAM	Constructed through data interpolation or calculated with land-sea breeze or complex terrain wind model.	3-D wind field. Finite difference numerical technique.	Vertical turbulent diffusion function of atmospheric stability and friction velocity. Constant horizontal turbulent diffusion coefficient.
CIT	Constructed through data interpolation with diagnostic wind model.	3-D wind field. Finite element numerical technique.	Vertical turbulent diffusion function of atmospheric stability and friction velocity. Horizontal turbulent diffusion function of mixing height and convective velocity scale.
ROM	Constructed through data interpolation.	3-D wind field with vertical transport through cumulus clouds. Finite difference numerical technique.	Vertical turbulent diffusion function of atmospheric stability. Horizontal turbulent diffusion function of atmospheric stability, convective cloud cover and velocity scale, and the depths of the boundary layer and clouds.
RADM	Calculated with Community Climate Model (CCM) and MM4.	3-D wind field with vertical transport through cumulus clouds. Finite difference numerical technique.	Vertical turbulent diffusion function of atmospheric stability and wind shear. No horizontal turbulent diffusion.
ADOM	Constructed through data interpolation in combination with prognostic planetary boundary-layer model.	3-D wind field with vertical transport through cumulus clouds. Cubic spline numerical technique.	Vertical turbulent diffusion calculated from planetary boundary layer model. No horizontal turbulent diffusion.
STEM-II	Calculated with dynamic wind model (MASS) or constructed through data interpolation.	3-D wind field with vertical transport through clouds. Finite element numerical technique.	Vertical turbulent diffusion function of atmospheric stability and surface roughness. Horizontal turbulent diffusion proportional to vertical turbulent diffusion.

[a]See Appendix A for abbreviations and acronyms.

Table 3-24 summarizes the gas-phase chemical mechanisms incorporated into the six models. Generally three chemical mechanisms are used in the models: (1) CBM-IV used in ROM and UAM; (2) versions of the SAPRC mechanism used in ADOM, STEM-II, and CIT; and (3) the RADM mechanism. Of the three chemical mechanisms, RADM is the largest and CBM-IV is the smallest. Aqueous-phase chemistry is currently treated only in the regional models. Cloud processes are treated in the three regional models, RADM, ADOM, and STEM-II (Table 3-25). Cumulus venting and solar attenuation are treated in ROM. Layer 3 depths also are influenced by cloud thickness. At present, only RADM, ADOM and STEM-II treat wet deposition. The treatment of dry deposition in the models also is summarized in Table 3-25.

Regional-scale modeling is an important contributor to the development of boundary conditions for urban-scale models. In recent years, regional-scale modeling has been receiving increased attention as the need for addressing interlinked air quality problems at broader scales is increasing. At the expanded spatial and temporal scales of regional-scale models, the simulation of certain dynamic processes becomes more critical. For example, in regional-scale models the treatment of biogenic VOC emissions and removal by dry and wet deposition generally require greater attention and accuracy than at the urban scale. On the other hand, the exact mechanistic details of the oxidation of some highly reactive VOCs may be somewhat less important.

More detailed descriptions now will be presented for UAM, ROM, and RADM. The UAM is described, as it is specified officially by EPA, as a grid-based model for urban-scale O_3 control strategy determination. The regional-scale O_3 model, ROM, is being used by EPA to evaluate O_3 control measures for the eastern United States and to provide boundary conditions for urban area simulations using UAM. Representative of a comprehensive state-of-the-science O_3/acid deposition model, RADM has been used to evaluate combined O_3 and acid deposition abatement strategies for the northeastern United States and Canada.

The EPA is embarking on a project to produce the next generation of photochemical models, termed MODELS 3 (Dennis et al., 1993b). This group of models will be flexible (scalable grid and domain), will be modular (modules with interchangeable data structure), will have uniform input/output across subsystems, and will contain advanced analysis and visualization features. The models will be designed to take advantage of the latest advances in computer architecture and software.

3.6.3.1 The Urban Airshed Model

The UAM is the most widely applied and broadly tested grid-based photochemical air quality model. The model is described in a number of sources, including a multi-volume series of documents issued by the U.S. Environmental Protection Agency (1990a,b,c; 1992b) and a comprehensive evaluation by Tesche et al. (1993). Current versions include provisions enabling the user to model transport and dispersion within both the mixed and inversion layers. The computer codes have been structured to allow inclusion of up to 10 vertical layers of cells and any number of cells horizontally.

The original UAM developed by Reynolds et al. (1973) simulated the dynamic behavior of six pollutants: (1) reactive and (2) unreactive hydrocarbons, (3) NO, (4) NO_2, (5) O_3, and (6) CO. Since 1977, the UAM has employed various versions of the CBM. Currently, the model utilizes the CBM-IV Mechanism (Gery et al., 1988, 1989), which treats

Table 3-24. Grid-based Urban and Regional Air Pollution Models: Treatment of Chemical Processes[a]

Model	Gas-Phase Chemistry	Aqueous- Phase Chemistry
UAM	Eighty-seven reactions among 36 species including NO_x, O_3, ROG, and SO_2 (CBM-IV) (Gery et al., 1988, 1989)	No treatment of aqueous-phase chemistry
CIT	One hundred and twelve reactions among 53 species including NO_x, O_3, ROG, and SO_2 (Lurmann et al., 1986)	No treatment of aqueous-phase chemistry
ROM	Eighty-seven reactions among 36 species including NO_x, O_3, ROG, and SO_2 (CBM-IV)	No treatment of aqueous-phase chemistry
RADM	One hundred and fifty-seven reactions among 59 species including NO_x, O_3, ROG, and SO_2 (Stockwell et al., 1990)	Forty-two equilibria and five reactions for SO_2 oxidation
ADOM	One hundred and twelve reactions among 53 species including NO_x, O_3, ROG, and SO_2 (Lurmann et al., 1986)	Fourteen equilibria and five reactions for SO_2 oxidation
STEM-II	One hundred and twelve reactions among 53 species including NO_x, O_3, ROG, and SO_2 (Lurmann et al., 1986)	Twenty-six equilibria and about 30 reactions for SO_2 and NO_x oxidation, radical chemistry, and transition metal chemistry

[a]See Appendix A for abbreviations and acronyms.

Table 3-25. Grid-based Urban and Regional Air Pollution Models: Treatment of Cloud and Deposition Processes[a]

Model	Cloud Processes	Wet Deposition	Dry Deposition
UAM	No treatment of cloud processes.	No treatment of wet deposition.	Dry deposition velocity approach; function of wind speed, friction velocity, land type, and species.
CIT	No treatment of cloud processes.	No treatment of wet deposition.	Dry deposition velocity approach; function of atmospheric stability, wind speed, land type, and species.
ROM	No treatment of cloud processes, except vertical transport treatment.	No treatment of wet deposition.	Resistance transfer approach; function of land type, wind speed, atmospheric stability, and species.
RADM	Treatment of precipitating cumulus clouds, precipitating stratus clouds, and fair-weather cumulus clouds, based on precipitation amount, temperature, and relative humidity vertical profiles. Use of cloud-averaged properties for aqueous chemistry.	Calculated from precipitation rate and cloud average chemical composition; no below-cloud scavenging.	Resistance transfer approach; function of atmospheric stability, wind speed, season, land type, insolation, surface wetness, and species.
ADOM	Treatment of cumulus clouds and stratus clouds, based on precipitation amount (for stratus clouds), temperature, and relative humidity vertical profiles. Vertical resolution for cloud chemistry.	Calculated from precipitation rate and vertically weighted cloud average chemical composition, below-cloud scavenging included.	Resistance transfer approach; function of atmospheric stability, wind speed, land type, season, insolation, and species.
STEM-II	Treatment of clouds with the Advanced Scavenging Module based on cloud-base height, precipitation rate, and surface temperature.	Calculated with the Advanced Scavenging Module. Treats cloud water, rain water, and snow; below-cloud scavenging included.	Resistance transfer approach; function of atmospheric stability, land type, wind speed, and species.

[a]See Appendix A for abbreviations and acronyms.

36 reacting species. Reactive organic compounds include alkanes, alkenes, aromatics, and aldehydes, and nitrogen-bearing species include HNO_2, HNO_3, and PAN.

Under development at the time of writing of the present document is version V of UAM (Morris et al., 1991, 1992). This version (UAM-V) contains the following features: the ability to treat two-way interactive nested grids; the use of state-of-the-science treatment of atmospheric, meteorological, and chemical processes; the treatment of subgrid-scale plume processes using a plume-in-grid algorithm; and the use of structured programming techniques to take advantage of computational speed enhancement opportunities offered by the current and next generation of computers.

3.6.3.2 The Regional Oxidant Model

The ROM was designed to simulate most of the important chemical and physical processes that are responsible for the photochemical production of O_3 over regional domains and for episodes of up to 15 days in duration. These processes include horizontal transport; atmospheric chemistry and subgrid-scale chemical processes; nighttime wind shear and turbulence associated with the low-level nocturnal jet; the effects of cumulus clouds on vertical mass transport and photochemical reaction rates; mesoscale vertical motions induced by terrain and the large-scale flow; terrain effects on advection, diffusion, and deposition; emissions of natural and anthropogenic O_3 precursors; and dry deposition. The processes are simulated mathematically in a three-dimensional Eulerian model with three vertical layers, including the boundary layer and the capping inversion or cloud layer. The ROM geographical domains are summarized in Table 3-26 and illustrated in Figure 3-26.

Meteorological data are used to model objectively both regional winds and diffusion. The three model layers of ROM are prognostic (predictive) and are free to expand and contract locally in response to changes in the physical processes occurring within the layers. During an entire simulation period, horizontal advection and diffusion and gas-phase chemistry are modeled in the three layers. Predictions from Layer 1 are used as surrogates for surface concentrations. Layers 1 and 2 model the depth of the well-mixed layer during the day. Some special features of Layer 1 include the modeling of the substantial wind shear that can exist in the lowest few hundred meters above ground in local areas where strong winds exist and the surface heat flux is weak, the thermal internal boundary layer that often exists over large lakes or near sea coasts, and deposition onto terrain features that protrude above the layer. At night, Layer 2 represents what remains of the daytime mixed layer. As stable layers form near the ground and suppress turbulent vertical mixing, a nocturnal jet forms above the stable layer and can transport aged pollutant products and reactants considerable distances. At night, emissions from tall stacks and warm cities are injected directly into Layers 1 and 2. Surface emissions are specified as a mass flux through the bottom of Layer 1. During the day, the top model layer, Layer 3, represents the synoptic-scale subsidence inversion characteristic of high O_3-concentration periods; the base of Layer 3 is typically 1 to 2 km above the ground. Relatively clean tropospheric air is assumed to exist above Layer 3 at all times, and stratospheric intrusion of O_3 is assumed to be negligible. If cumulus clouds are present, an upward flux of O_3 and precursor species is injected into the layer by penetrative convection. At night, O_3 and the remnants of other photochemical reaction products may remain in this layer and be transported long distances downwind. These processes are modeled in Layer 3.

When cumulus clouds are present in a Layer 3 cell, the upward vertical mass flux from the surface is partially diverted from injection into Layer 1 to injection directly into the

Table 3-26. Regional Oxidant Model Geographical Domains

GENERAL INFORMATION

    ROM grid cells are 1/4° longitude and 1/6° latitude in size or approximately 18.5 km. Actual domain names are included in parenthesis after the general geographical description. In addition, all domains can be run independently or windowed from the "super" domain.

SUPER DOMAIN (SUPROXA)
    99.00 W to 67.00 W Longitude
    26.00 N to 47.00 N Latitude
    128 × 126 Grid Cells (columns × rows)

SOUTHERN DOMAIN (TEXROXA)
    99.00 W to 81.00 W Longitude
    26.00 N to 37.67 N Latitude
    72 × 70 Grid Cells (columns × rows)

NORTHEAST DOMAIN (NEROXA)
    89.00 W to 67.00 W Longitude
    35.00 N to 47.00 N Latitude
    88 × 72 Grid Cells (columns × rows)

NORTHEAST DOMAIN (ROMNET)
    85.00 W to 69.00 W Longitude
    36.33 N to 45.00 N Latitude
    64 × 52 Grid Cells (columns × rows)

MIDWEST DOMAIN (MIDROXA)
    97.00 W to 78.00 W Longitude
    35.00 N to 47.00 N Latitude
    76 × 72 Grid Cells (columns × rows)

NORTHEAST DOMAIN (NEROS1)
    84.00 W to 69.00 W Longitude
    38.00 N to 45.00 N Latitude
    60 × 42 Grid Cells (columns × rows)

SOUTHEAST DOMAIN (SEROXA)
    98.75 W to 76.25 W Longitude
    27.67 N to 37.67 N Latitude
    90 × 60 Grid Cells (columns × rows)

SOUTHEAST DOMAIN (SEROS1)
    97.00 W to 82.00 W Longitude
    28.00 N to 35.00 N Latitude
    60 × 42 Grid Cells (columns × rows)

cumulus cloud of Layer 3. In the atmosphere, strong thermal vertical updrafts, primarily originating near the surface in the lowest portion of the mixed layer, feed growing "fair-weather cumulus" clouds with vertical air currents that extend in one steady upward motion from the ground to well above the top of the mixed layer. These types of clouds are termed fair-weather cumulus because atmospheric conditions are such that the clouds do not grow to the extent that precipitation forms. The dynamic effects of this transport process and daytime cloud evolution can have significant effects on the chemical fate of pollutants. Within the ROM system, a submodel parameterizes the above-cloud flux process and the subsequent impact on mass fluxes among all layers of the model. In the current implementation of the chemical kinetics, liquid-phase chemistry is not included, and, thus, part of the effects from the cloud flux processes are not accounted for in the simulations. The magnitude of the mass flux proceeding directly from the surface layer to the cloud layer is modeled as being proportional to the observed amount of cumulus cloud coverage and inversely proportional to the observed depth of the clouds.

       Horizontal transport within the ROM system is governed by hourly wind fields that are interpolated from periodic wind observations made from upper-air soundings and
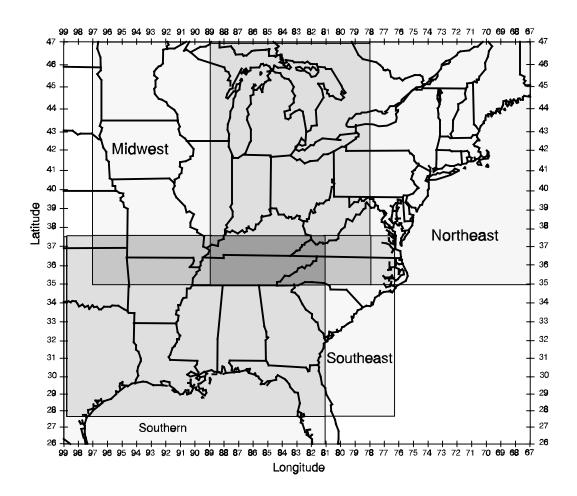
Figure 3-26. Regional oxidant model superdomain with modeling domains.

surface measurements. During the nighttime simulation period, the lowest few hundred meters of the atmosphere above the ground may become stable as a radiation inversion forms. Wind speeds increase just above the top of this layer, forming the nocturnal jet. This jet is capable of carrying O_3, other reaction products, and emissions injected aloft considerable distances downwind. This phenomenon is potentially significant in modeling regional-scale air quality and is implicitly treated by the model, where the definition of Layer 1 attempts to account for it.

The ROM system requires five types of "raw" data inputs: (1) air quality, (2) meteorology, (3) emissions, (4) land use, and (5) topography.

Air quality data required by the ROM include initial conditions and boundary conditions. The model usually is initialized 2 to 4 days before the start of the period of interest with clean tropospheric conditions for all species. This period of interest is called an "episode" and usually lasts around 15 days. Ideally, the initial condition field will have been transported out of the model domain in advance of the portion of the episode of greatest interest. Upwind lateral boundary conditions for O_3 are updated every 12 h based on measurements, except for the large superdomain, where tropospheric background values are